Early-life stress alters postnatal chromatin development in the nucleus accumbens

Rebekah L. Rashford[1], Michael DeBerardine[1], Hye Ji J. Kim[1], Nibal Arzouni[1,2], Laura W. Hirschfield[1], Oluwamayowa M. Oke[1], Shannon N. Bennett[1], Catherine Jensen Peña[1]*

ABSTRACT:

Early-life stress sensitizes individuals to subsequent stressors to increase lifetime risk for psychiatric disorders. Within the nucleus accumbens (NAc) — a key limbic brain region — early-life stress sensitizes both cellular and transcriptional response to later stress. However, the molecular mechanisms linking initial activation of neurons by early-life stress with continued stress sensitivity across the lifespan are poorly understood. Using a combination of activity-dependent cellular tagging and ATAC-sequencing across postnatal development, we find that early-life stress initially opens chromatin in stress-activated cells and that chromatin opening predicts gene expression response to adult stress, suggesting epigenetic priming as a mechanism of stress sensitization. Moreover, early-life stress accelerates both chromatin development within these activated cells, and H3K4me1 deposition broadly in NAc — a post-translational histone modification associated with open chromatin and epigenetic priming. By adulthood, we observe chromatin remodeling throughout the NAc, indicating that the effects of stress are long-lasting and propagate across development into the broader cell population. Lastly, through viral-mediated epigenome editing and behavioral quantification, we find that deposition of H3K4me1 in NAc during early postnatal development is sufficient to mimic early-life stress and prime hypersensitivity to subsequent stress. Together, our results show that a molecular memory of early-life stress is encoded at an epigenetic level through changes in chromatin architecture. This constitutes a novel biological mechanism by which early-life stress programs lifelong stress sensitivity.

INTRODUCTION

Millions of children worldwide experience early-life stress (ELS), which increases lifetime risk for developing mood, anxiety, and substance use disorders (Green et al., 2010; Kessler et al., 2010; Kendler et al., 2011; Scott et al., 2012). ELS broadly encompasses many adverse experiences including maltreatment (neglect, and/or physical, sexual, and/or emotional abuse), death or loss of a caregiver, poverty, systemic racism, exposure to community violence, or experience of a natural disaster (Hackman et al., 2010; UNICEF, 2018; Giano et al., 2020; Sisk et al., 2023; Webb et al., 2024). Studies in humans and preclinical animal models have shown that ELS sensitizes individuals to future stressors, which may be at the root of increased psychiatric disease risk (McLaughlin et al., 2010; Zhang et al., 2016; Peña et al., 2017; Saxton and Chyu, 2019; Sidamon-Eristoff et al., 2022).

ELS alters function and regulation of the nucleus accumbens (NAc) (Hanson et al., 2021), a ventral striatal brain region extensively implicated in the pathophysiology of psychiatric disease (Russo and Nestler, 2013). In children, ELS alters development and connectivity of the ventral striatum, and changes in NAc activity are associated with blunted reward processing, anhedonia, and heightened response to stressors (Hanson et al., 2015, 2016, 2018; Kirshenbaum et al., 2024). At a cellular level, ensembles of NAc neurons initially activated by experience of ELS are hyper-reactive to stress across the lifespan, contributing to stress sensitivity in mice (Balouek et al., 2023). Interestingly, ELS-activated neurons are not hyperactive in the absence of additional stress. This indicates a latent hypersensitivity to stress which may be encoded at a molecular level within this ELS-responsive cell population (Josselyn et al., 2015).

At a transcriptional level, ELS induces both long-lasting changes to baseline gene expression, and latent gene expression changes revealed by a second hit of stress in adulthood (Peña et al., 2019b), pointing to epigenetic regulatory mechanisms. While experience of ELS can alter histone variants and post-translational histone modifications in brain reward circuitry

[1] Princeton Neuroscience Institute, Princeton University, Princeton, NJ 08544, USA
[2] Lewis Sigler Institute of Integrative Genomics, Princeton University, Princeton, NJ 08544, USA
* *Correspondance to: Catherine J. Peña (cpena@princeton.edu)*

(Lepack et al., 2016; Kronman et al., 2021; Torres-Berrío et al., 2023; Geiger, Balouek et al., 2024), it is unknown whether ELS indeed primes chromatin architecture in the NAc to facilitate or sensitize transcriptional response to subsequent stressors. Here, we sought to determine whether ELS alters the chromatin landscape in ELS-activated cells during postnatal development, investigating the degree, timing, and endurance of such architectural changes, and whether such chromatin changes were functionally relevant for response to future stress. Our results provide novel insights into how the epigenome encodes long-lasting stress sensitivity.

RESULTS

Tagging and capturing stress-responsive and non-responsive cells of the NAc

Given previous findings that ELS-activated cells in the NAc are preferentially reactivated by stress (Balouek et al., 2023), we examined chromatin profiles in ELS-activated and non-activated cell populations separately. To permanently tag and isolate these separate cell populations, we utilized double transgenic *ArcCreER^{T2} x Sun1-sfGFP-Myc* mice (**Figure 1A**) in which transgene expression is both neuronal activity- and ligand-dependent (Denny et al., 2014; Balouek et al., 2023). ELS occurred in a stress sensitive window from postnatal day P10-17 as previously described (Peña et al., 2017, 2019a). Genetic recombination was induced on P17 by administration of 4-OHT either at the beginning of a period of maternal separation (ELS) or exploration of an enrichment object (standard-reared pups, Std) (**Figure 1B**). Permanent expression of nuclear membrane-localized SUN1-sfGFP-Myc (**Figure 1C and D**) enabled us to affinity-purify tagged nuclei within four days after recombination (P21) or later in adulthood (>P60; **Figure 1B**) by the INTACT method (Deal and Henikoff, 2010; Mo et al., 2015). Both male and female samples were collected from each group at each age. For both Std and ELS groups, approximately 10% of nuclei in the NAc were tagged and captured (**Figure 1E**), consistent with previous count estimates of experience-activated cells by immunohistochemistry (Balouek et al., 2023). We then performed ATAC-sequencing (assay for transposase-accessible chromatin; (Buenrostro et al., 2013) in both tagged and untagged cell populations to characterize and compare open chromatin regions across treatment conditions and cell populations (**Supplemental Table 1**). We further validated that experience-activated cells have open chromatin peaks at the *Arc* gene promoter used to drive transgene expression, in both Std and ELS samples, thus demonstrating the potential for these cells to have been activated (**Figure 1F**).

ELS opens chromatin in experience-activated cells of the NAc following stress

Among experience-activated NAc cells, we identified 150,895 total accessible regions of chromatin (**Figure 2A**). In the non-activated cells, we found 108,286 total ATAC peaks. To determine how chromatin is remodeled in the aftermath of ELS, we calculated differences in chromatin accessibility (differentially accessible regions (DARs); p-value<0.01 and |logFC|>1.5; **Figure 2 B-D**) at P21 between ELS and Std samples in both experience-activated and non-activated cells. Within experience-activated cells, we identified 348 genomic regions opened by ELS and 100 genomic regions closed by ELS (**Figure 2B, D**), such that the predominant response to ELS was to open chromatin. In contrast, within non-activated cells, we found minimal effect of ELS wherein ELS impacted a total of 56 regions (**Figure 2C**), demonstrating that the immediate impact of ELS is within ELS-activated cells.

We next sought to characterize these activated-cell DARs to better understand how ELS alters gene regulatory functions and biological processes. Both open and closed

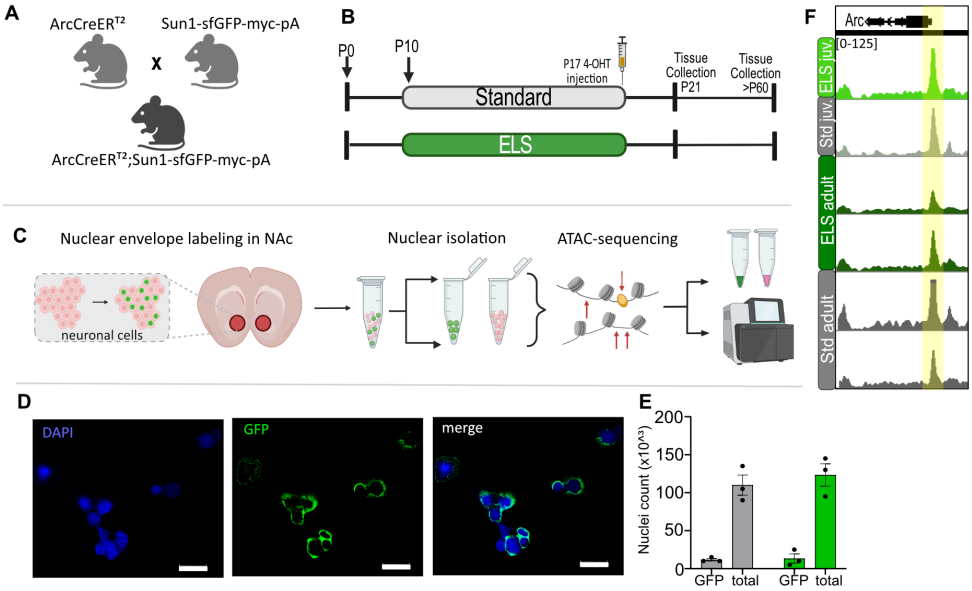

Figure 1 | Tagging and capturing stress-responsive and non-responsive cells of the NAc. (A) Breeding scheme of *ArcCreER^{T2} x Sun1-sfGFP-Myc* mice. **(B)** Experimental timeline for ELS from P10-17, 4-OHT -induced recombination at P17 in standard-reared (Std) and ELS pups, and tissue collection at either P21 or >P60 in adulthood. **(C)** Schematic of 4-OHT- and activity-dependent recombination and tagging of NAc neurons, followed by nuclear isolation, affinity-purification of tagged cells, and ATAC-sequencing and analysis in both tagged and untagged cells. **(D)** Example images of purified nuclei expressing SUN1-GFP in the nuclear membrane (scale bar 25 µm). **(E)** Average counts of total and affinity-purified (GFP) nuclei from standard-reared (gray) and ELS (green) samples. Error bars are mean±SEM. **(F)** Example browser tracks of ATAC peaks at the *Arc* promotor from experience-activated samples.

DARs were enriched for 3'UTRs, 5'UTRs, exons, introns, and enhancer genomic features compared to expected proportions of the mouse genome (**Figure 2E**). However, in contrast to putative enhancer regions, proximal promoter and intergenic regions were underrepresented among DARs. Overall, 94-95% of opened and closed DARs from the activated population were in putative cis-regulatory elements, defined as >1kb from the nearest transcription start site, as enhancers may also be found within intronic, exonic, and intergenic regions (**Figure 2F;** (Moore et al., 2020). The relatively small fraction of DARs within promoter regions suggests that changes to gene transcription following ELS are generally not associated with changes to promoter accessibility, but rather functional changes at long-range cis-regulatory elements that in turn modulate the frequency of transcription at their target genes. Given an enrichment of DARs within putative cis-regulatory regions of activated cells, we next sought to identify what genes and functions these loci regulate. While many enhancers regulate their nearest gene neighbor, enhancers can also regulate genes hundreds of kilobases away (Schoenfelder and Fraser, 2019). We therefore mapped putative long-range interactions between DARs and predicted target genes using publicly available Hi-C data from mouse brains (Deng et al., 2015; O'Connor et al., 2020; Reiff et al., 2022) and performed gene ontology enrichment analysis for biological processes associated with the putatively contacted genes (**Figure 2G-H**). Genes in, or putatively contacted by, open DARs were enriched for functions related to transcription, response to stimulus, development, and cellular metabolism (**Figure 2H**, left). Genes in or putatively contacted by closed DARs were enriched for functions related to JAK-STAT signaling, signal transduction, proliferation, and regulation of cell communication (**Figure 2H**, right).

To determine whether DARs were enriched for any functional elements such as transcription factor binding

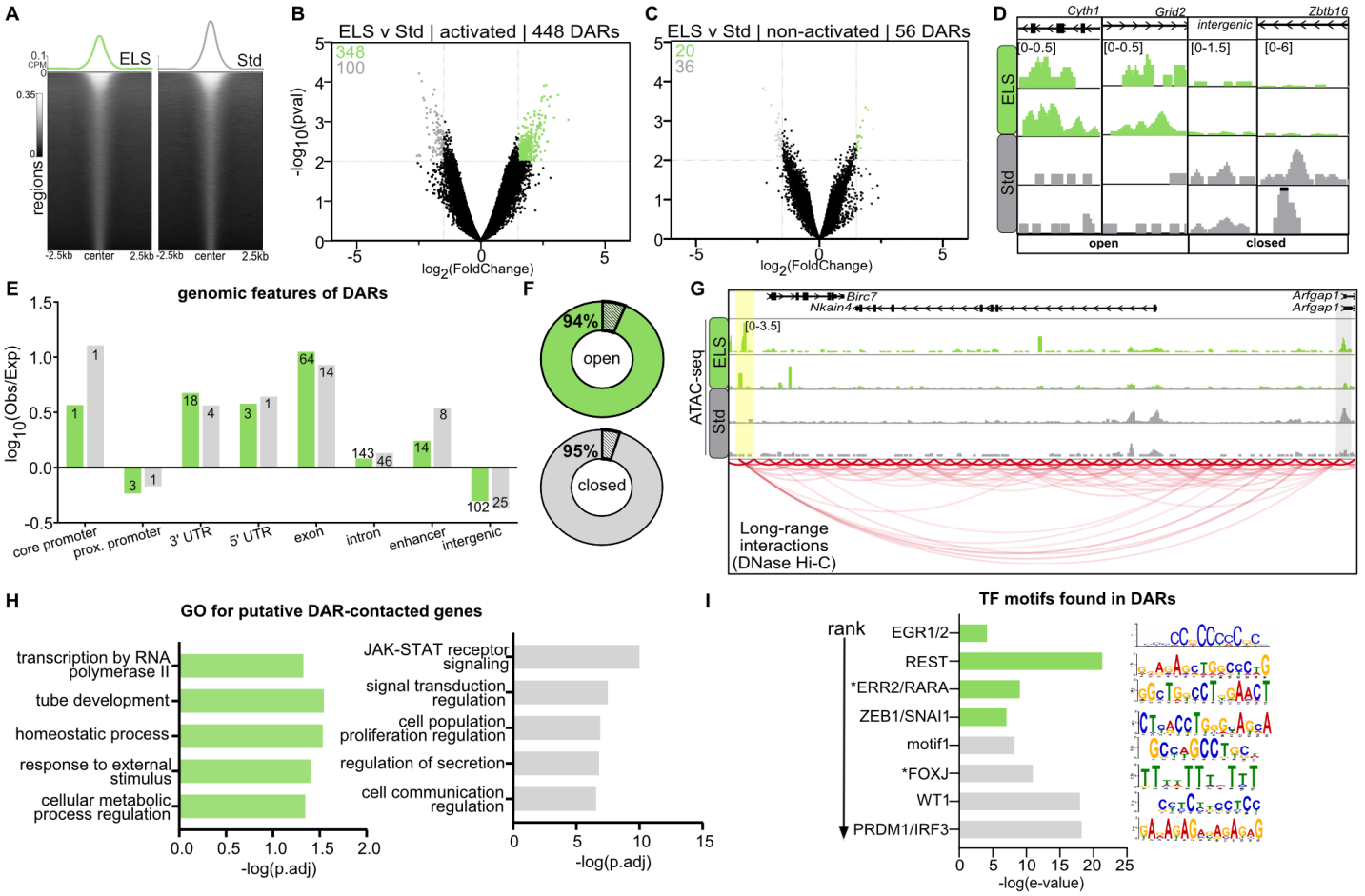

Figure 2 | ELS opens chromatin in experience-activated cells of the NAc following stress.
(A) Line plots (top) and heatmaps (bottom) of mean chromatin accessibility CPM ±2.5 kb around center of all ATAC peaks within experience-activated cells. Volcano plot of ELS vs Std differentially accessible regions (DARs) within P21 experience-activated **(B)** and P21 non-activated **(C)** cells. Differentially accessible regions (DARs: edgeR, *p*-value <0.01 and |logFC|>1.5) opened or closed by ELS in are shown in green and gray, respectively. **(D)** Example browser tracks of ATAC peaks either opened or closed by ELS in P21 experience-activated cells, normalized to CPM. **(E)** Count and enrichment or depletion ($\log_{10}$ of observed over expected for each genomic feature in the mm10 genome) of DARs mapped to each genomic feature for regions opened (green) or closed (gray) by ELS within experience-activated samples. **(F)** Proportion of DARs in putative cis-regulatory elements (>1kb from the nearest TSS) for regions opened (green) or closed (gray) by ELS within experience-activated samples. **(G)** Example browser tracks and long-range interactions between an open DAR (yellow highlight) and a putative target gene promoter (gray highlight). **(H)** Gene Ontology (GO) biological process terms for genes putatively contacted by ELS-opened (green) or closed DARs. **(I)** Top transcription factor motifs found in open (green) and closed (gray) DARs ; * denotes motifs found in <60% of input regions.

sites, we performed motif analysis (Grant and Bailey, 2021). Genomic loci that gained ATAC peaks after ELS were enriched for binding sites for EGR1/2, REST, ERR2/RARA, and ZEB1/SNAI1, indicating that ELS alters transcriptional regulation and response to stimuli (**Figure 2I;** Bading et al., 1995; Schoenherr and Anderson, 1995; Ana Maria et al., 2015; Wu et al., 2017; Wang et al., 2019; Godino et al., 2023). Genomic loci that lost ATAC peaks after ELS were enriched for a novel motif and binding sites for FOXJ, WT1, and PRDM1/IRF3, indicating that ELS may close regions that regulate developmental programs and immune response (**Figure 2I;** Taniguchi et al., 2001; Hannenhalli and Kaestner, 2009; Wurst and Prakash, 2014; Kusiak and Brady, 2022). Taken together, these results demonstrate that ELS largely opens chromatin in NAc, that chromatin remodeling is specific to ELS-activated cells and persists for at least several days, and that such remodeling may serve to alter transcriptional response to stimulus.

ELS impacts chromatin accessibility across a broad NAc cell population over time

In order to determine whether these near-term changes in chromatin persist into adulthood, we compared the differential accessibility profiles between the ELS and Std-reared conditions in adulthood using the same total ATAC peak sets from the experience-activated and non-activated cells. As described above, we identified a total of 108,286 ATAC peaks within the non-activated cells (**Figure 3A**). In contrast to the chromatin opening observed at P21 in ELS-activated cells, there were no DARs in adult experience-activated cells (**Figure 3B**). Instead, there were 390 opened and 594 closed regions in cells that were not initially activated in response to ELS (**Figure 3C-D**), indicating that the effect of ELS propagated across development into the broader NAc cell population.

We therefore characterized these opened and closed regions within initially-non-activated cells from adult NAc.

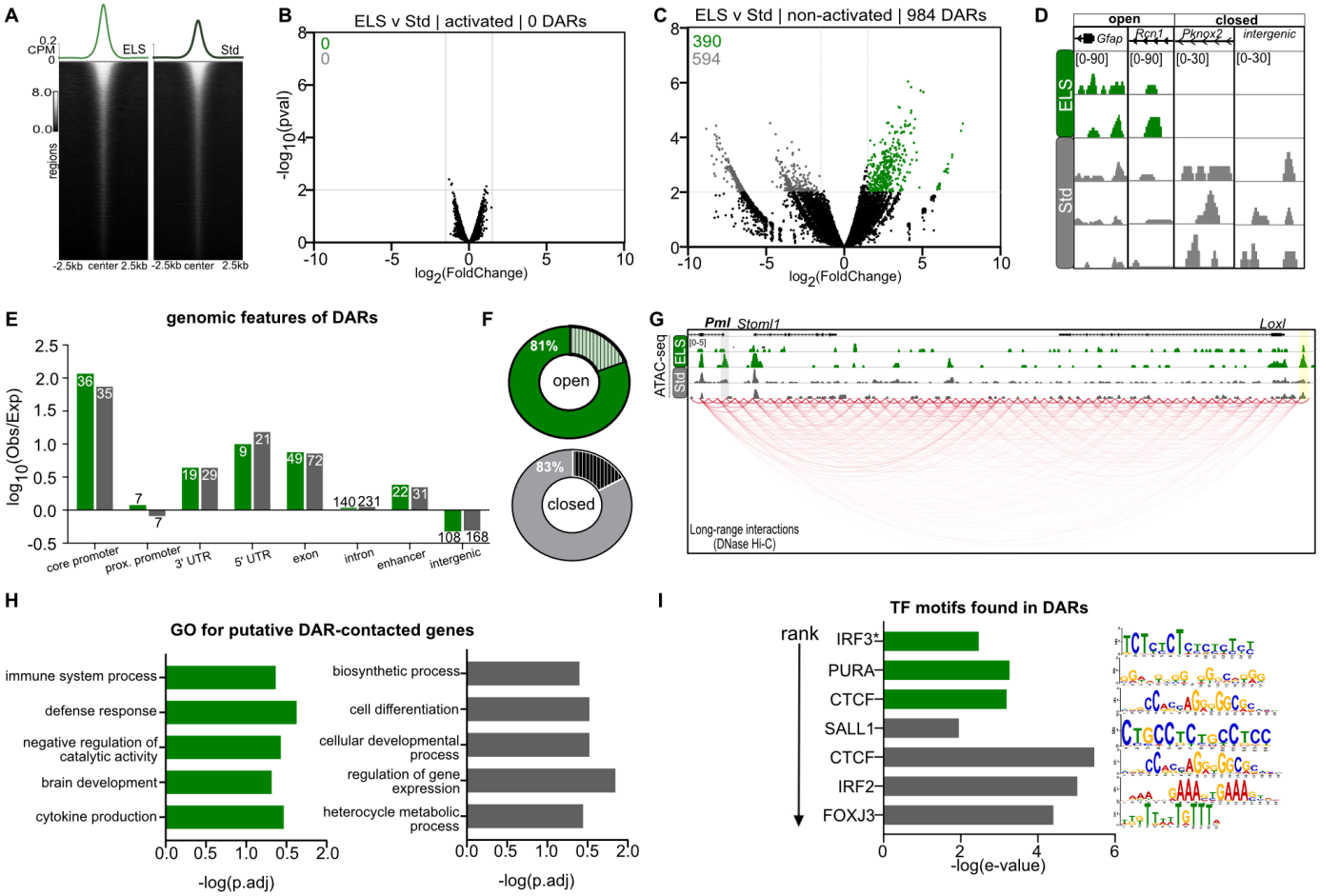

Figure 3 | ELS impacts chromatin accessibility across a broad NAc cell population over time.
(A) Line plots (top) and heatmaps (bottom) of mean chromatin accessibility CPM ±2.5 kb around center of all ATAC peaks within non-activated cells. Volcano plot of ELS vs Std differentially accessible regions (DARs) within adult experience-activated **(B)** and adult non-activated **(C)** cells. Differentially accessible regions (DARs: edgeR, *p*-value<0.01 and |logFC|>1.5) opened or closed by ELS are shown in green and gray, respectively. **(D)** Example browser tracks of ATAC peaks either opened or closed by ELS in experience-activated cells normalized to CPM. **(E)** Count and enrichment or depletion (log_{10} of observed over expected for each genomic feature in the mm10 genome) of DARs mapped to each genomic feature for regions opened (green) or closed (gray) by ELS within experience-activated samples. **(F)** Proportion of DARs in putative cis-regulatory elements (>1kb from the nearest TSS) for regions opened (green) or closed (gray) by ELS within experience-activated samples. **(G)** Example browser tracks and long-range interactions between an open DAR (yellow highlight) and a putative target gene promoter (gray highlight). **(H)** Gene Ontology (GO) biological process terms for genes putatively contacted by ELS-opened (green) or closed DARs. **(I)** Top transcription factor motifs found in open (green) and closed (gray) DARs ; * denotes motifs found in <60% of input regions.

Adult DARs both opened and closed by ELS were enriched for nearly all genomic features except intergenic regions, which were depleted (**Figure 3E**), and were largely in putative cis-regulatory elements (81-83% of DARs; **Figure 3F**). As with juvenile peaks, we mapped putative long-range interactions and performed gene ontology analysis in order to identify what genes and functions these loci may regulate (**Figure 3G-H**). Genes within — or putatively contacted by — open DARs were enriched for functions related to immune system processes and brain development, while closed-DAR-contacted genes regulated biosynthetic processes, cellular differentiation and development, and gene expression (**Figure 3H**).

Similar to juvenile motif enrichment, genomic loci that decreased in accessibility by adulthood after ELS were enriched for binding sites for transcription factors in the FOXJ and IRF families (**Figure 3I**), demonstrating that some changes in these transcription factor programs persist across development. Genomic loci that gained accessibility in adulthood after ELS were enriched for transcription factor binding sites implicated in immune response pathways (IRF3 and PURA) (**Figure 3I**; Gallia et al., 2000; Taniguchi et al., 2001; Khalili et al., 2003; Johnson et al., 2006). Interestingly, DARs that both gained and lost accessibility after ELS were enriched for CTCF motifs. CTCF is an architectural protein which facilitates enhancer-promoter interactions through three-dimensional chromatin looping (Ong and Corces, 2014), supporting the hypothesis that ELS may alter genomic architecture to impact long-range transcriptional regulation.

While cell-type specificity is obscured by semi-bulk ATAC-seq, we examined enrichment of ATAC peaks in promoters of genes marking different canonical cell types found within the NAc to estimate relative proportions of previously-identified NAc cell types (**Supplemental Figure 1A-J**). Experience-activated cells from Std and ELS NAc included open chromatin at both the *Drd1* and *Drd2* promoters (**Supplemental Figure 1B**). This is consistent with findings that both classes of medium spiny neurons are altered by stress and engaged by both positive and negative valence stimuli (Francis et al., 2014; Peña, 2017; Zachry et al., 2024). Experience-activated cells also included open chromatin at the promoter for *Grm8* promoter (**Supplemental Figure 1I**), which encodes a metabotropic glutamate receptor and marks a distinct population of NAc medium-spiny neurons (Savell et al., 2020). Within experience-activated cells, little open chromatin was found within promoters of other neuronal population markers including *Drd3*, *Pdyn*, *Pvalb*, or *Chat* (Savell et al., 2020). Juvenile and adult non-activated cells from both Std and ELS NAc also included open chromatin peaks at *Drd1, Drd2*, and *Grm8* promoters as expected, as well as other neuronal (*Pdyn* and *Pvalb*) and non-neuronal (*Mog, Aqp4*, and *Cx3cr1*) markers examined, reflective of the fact that 90% of NAc cells were not activated and tagged (**Figure 1E**). However, adult ELS cells that were not initially activated had relatively greater ATAC peaks at promoters for *Mog* (marking oligodendrocytes) and *Cx3cr1* (marking microglia) and lower peaks within *Aqp4* (marking astrocytes) relative to Std-reared and juvenile samples (**Supplemental Figure 1F-H**). The finding that ELS alters chromatin in these cell populations that were not initially activated by ELS is consistent with research demonstrating dynamic cross-talk between neurons and glial cells, and that activity within non-neuronal cells adjacent to experience-activated neurons is required for long-term experience encoding (Badimon et al., 2020; Sun et al., 2024).

ELS accelerates normal chromatin development in experience-activated cells

Recent work has shown that enhancer usage continues to change between rodent postnatal weeks 1-3 as neurons mature (Stroud et al., 2020). To identify how chromatin changes across normal development in NAc, we performed differential accessibility analysis between juvenile and adult samples from standard-reared mice. Within experience-activated cells, chromatin accessibility largely decreased, with 536 regions closing and 130 regions opening from P21 to adulthood (**Figure 4A**). This is reminiscent of widespread decommissioning of enhancers that drive genes involved in neuronal proliferation and migration during early development (Stroud et al., 2020). Among non-activated cells, chromatin accessibility largely increased into adulthood, with 219 regions closing and 609 regions opening (**Supplemental Figure 2A**). This is consistent with earlier work showing that overall more enhancers become activated than repressed across later stages of postnatal development (Stroud et al., 2020; Ramirez et al., 2022).

Given that the ELS sensitive period from P10-17 overlaps with a postnatal period of enhancer maturation – and that enhancer maturation is modulated by neuronal activity and experience during this period (Stroud et al., 2020) – we hypothesized that ELS may disrupt postnatal chromatin maturation. To determine whether ELS alters the timing of chromatin maturation, we compared normalized chromatin accessibility counts within these standard opening and closing regions using a linear mixed effects model to account for sex and shared variance within individuals. By comparing the rate of chromatin maturation in ELS versus Std samples across time, we were also able to distinguish between three possibilities for how ELS opens chromatin following stress: 1) that ELS blunts closing of regions that should normally close during development, leaving chromatin in a more open, immature state; 2) that ELS aberrantly opens chromatin *de novo*, potentially through recruitment of pioneer factors; and 3) that ELS accelerates chromatin maturation such that

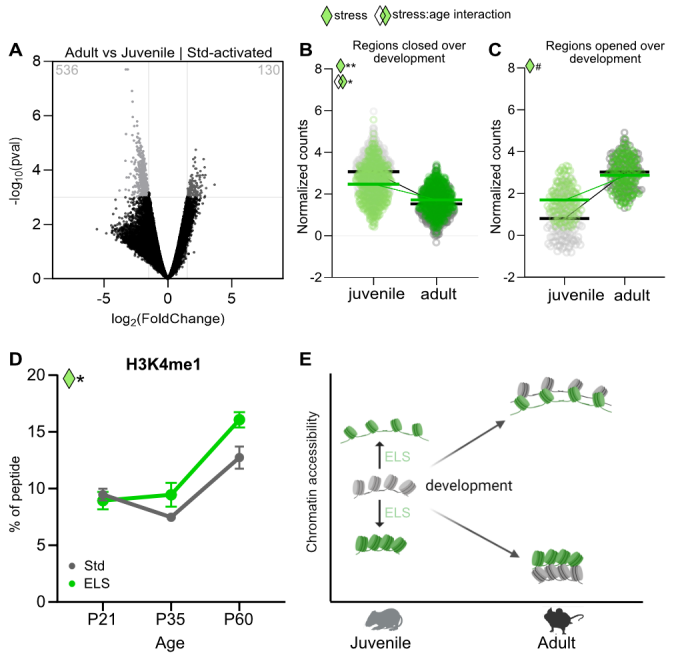

Figure 4 | ELS accelerates normal chromatin development in experience-activated cells. **(A)** Volcano plot of adult vs juvenile differentially accessible regions (DARs: edgeR, *p*-value<0.001 and |logFC|>1.5) within standard-reared experience-activated NAc samples. TMM-normalized counts of regions significantly closed **(B)** or opened **(C)** from P21 to adulthood among Std samples (gray) overlaid with normalized counts from the same regions among ELS samples (green). Main effects of and interactions between ELS and age are denoted (bars at mean; $^{**}p<0.01$; $^{*}p<0.05$; $^{\#}p<0.1$). **(D)** Proportion of monomethylated histone-3 lysine-4 peptide fragments in male NAc across postnatal development (mean±SEM; reanalyzed mass spectrometry data published in Kronman et al, *Nature Neuroscience*, 2021). **(E)** Schematic of the impact of ELS on chromatin architecture across postnatal development.

genomic loci set to open normally, open earlier. As expected, all analyses had a main effect of age (**Supplemental Table 2**). Sex was not a significant factor in any analysis. Among chromatin regions that close across standard development within experience-activated cells, there was a main effect of ELS [β= -0.874, SE=0.272, *p*=0.008] and an interaction between ELS and age [β=0.912, SE=0.338, *p*=0.021], such that closing regions were already more closed by P21 (**Figure 4B**). Similarly, among chromatin regions that open across standard development within experience-activated cells, there was a trend for a main effect of ELS [β=0.873, SE=0.469, *p*=0.089], such that opening regions were already more open by P21 (**Figure 4C**). These effects were specific to experience-activated cells (**Supplemental Figure 2B-C**). Together, these results demonstrate that ELS accelerates chromatin maturation in ELS-responsive cells. These findings of accelerated chromatin maturation also resolve the earlier puzzling results regarding the lack of differences in chromatin accessibility in adult experience-activated cells, reflecting a change in timing rather than location of chromatin remodeling.

We next asked whether ELS accelerates other aspects of chromatin development. We took advantage of published data that used mass-spectrometry to profile more than 200 individual and combinatorial post-translational histone modifications in the NAc at P21, P35, and P70-80 following ELS (Kronman et al., 2021). Interestingly, we found evidence for accelerated development of histone-3 lysine-4 monomethylation (H3K4me1) in the NAc (**Fig. 4D**; [main effect of ELS: F(1,12)=6.971, *p*=0.023; main effect of age: F(1,12)=35.53, *p*<0.0001; trending interaction: F(1,12)=3.498, *p*=0.067]). H3K4me1 is associated with open chromatin at gene promoters and enhancers, and marks primed enhancers in the absence of H3K4me3 and H3K27Ac (Calo and Wysocka, 2013). However, there were no main effects or interactions with ELS for H3K4me2, H3K4me3, or H3K27Ac, which are associated with active gene expression (**Supplemental Figures 3B-C**), suggesting that H3K4me1 differences following ELS may be specific to enhancer priming. We also found an interaction between ELS and age for H3K27me2, a histone modification associated with enhancer regulation (Ferrari et al., 2014), such that this modification was decreased following ELS but elevated in adulthood [**Supplemental Figure 3D**; F(1, 12)=5.874, *p*=0.017]. There were no main effects or interactions with ELS for H3K27me3 or H3K36me3, both associated with inhibition of gene expression (**Supplemental Figures 3E-F**). Taken together, our findings of accelerated chromatin maturation and accelerated H3K4me1 accumulation in the NAc, without simultaneous changes in markers of active gene expression, are consistent with premature development and priming of chromatin architecture (**Figure 4E**).

Chromatin opening after ELS predicts gene expression response to adult stress

An important question is whether the observed changes in chromatin accessibility after ELS are relevant to gene expression. Given an enrichment of DARs within putative cis-regulatory regions (**Figures 2G** and **3G**) and histone modifications associated with enhancer priming (**Figure 4E**), we speculated that chromatin changes may govern transcriptional response to future stress, in addition to the long-lasting changes to gene expression following ELS that we previously observed (Peña et al., 2019b). We first determined whether any DARs or genes putatively regulated by DARs (based on long-range interaction mapping) were maintained across development in activated and non-activated cell populations. None of the DARs from activated juvenile cells overlapped with DARs from non-activated adult cells. However, 37 genes putatively regulated by open DARs from each condition overlapped, and 37 genes putatively regulated by regions closed by ELS in both conditions overlapped (**Figure 5A**; **Supplemental Table 3**). This indicates that even though the impact of ELS on chromatin accessibility is dynamic across time and cellular populations, there is some consistency in the functional effect at the level of gene

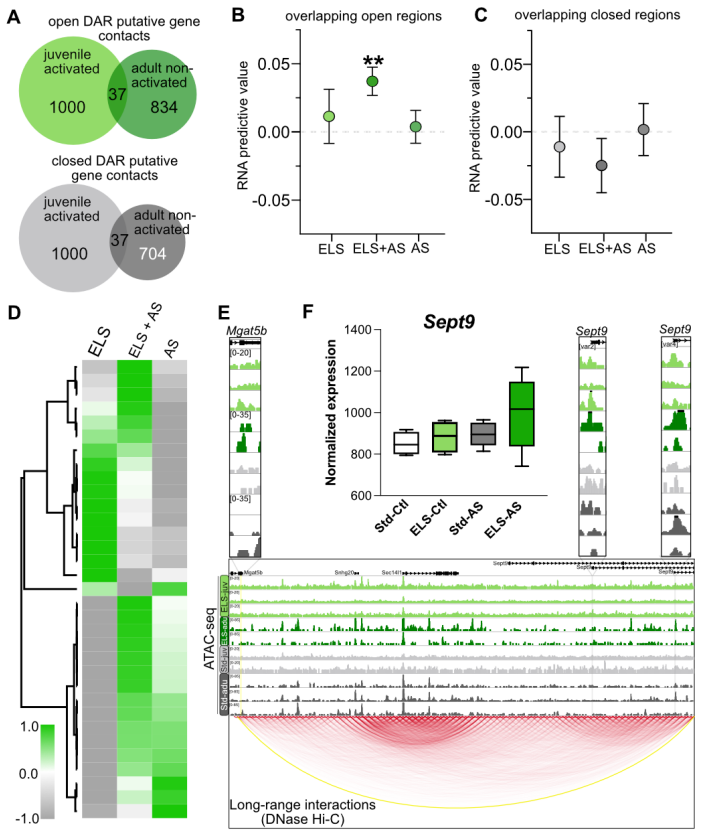

Figure 5 | Chromatin opening after ELS predicts gene expression response to adult stress.
(A) Venn diagrams showing overlap of genes putatively contacted by ELS-opened or ELS-closed DARs from P21 and adult samples (maximum predicted gene contacts limited to 1000). Measure of how well **(B)** open or **(C)** closed DARs predict NAc gene expression after ELS alone, ELS with a second hit of stress (ELS+AS), or adult stress (AS) alone, with positive values representing greater congruent prediction (mean±SEM, $^{**}p<0.01$). **(D)** Heatmap of expression changes of 37 genes contacted by open juvenile and adult DARs (row-normalized DESeq2 $\log_2$(FoldChange) values from ELS, ELS+AS, or AS, each vs Std-reared; hierarchically clustered). **(E)** Example browser tracks and long-range interactions between an opened DAR (yellow highlight) and a putative target gene, *Sept9* (gray highlight). **(F)** Boxplots of *Sept9* gene expression (CPM) among Std control, ELS control, Std+AS, or ELS+AS groups (min to max and mean represented) as an example. All gene expression data reanalyzed from adult male NAc RNA-seq published in Peña et al., *Nature Communications*, 2019; GEO GSE89692.

regulation.

Using previously published RNA-seq data from adult male NAc (Peña et al., 2019b), we mapped the expression changes of the putatively-contacted genes after different stress experiences: ELS, ELS + adult social defeat stress, or adult social defeat stress alone, compared to Std controls (**Figure 5D, 5F**). We calculated an "RNA predictive value" of chromatin opening or closing to predict increased or decreased expression, respectively, based on direction, magnitude, and significance of differential gene expression for each gene. Chromatin opening by ELS only had predictive value for the two-hit stress (ELS+adult stress) experience [two-tailed one-sample t-test: $t(1,30)=3.583$, $p=0.0012$; **Figure 5B**], but not to ELS or adult stress alone. Chromatin closing by ELS was not significantly predictive of RNA expression for any group (**Figure 5C**). We also found that among a subset of genes (e.g., *Sept9)*, there is an increase in expression in response to adult stress only if previously primed by ELS (**Figure 5F**). These results indicate that long-lasting increases in chromatin accessibility induced by ELS can predict transcriptional responses to adult stress later in life, consistent with the concept of epigenetic priming.

Epigenetic priming via postnatal H3K4me1 enrichment in NAc increases sensitivity to future stress

To test whether aberrant chromatin opening primes future stress response, we manipulated chromatin during postnatal development and tested behavioral sensitivity to adult stress. Because we found that ELS predominately opened chromatin within activated neurons after stress, which ultimately led to aberrant chromatin changes within the broader NAc cellular population in adulthood, we sought to widely deposit a histone modification associated with open chromatin, agnostic to neuronal activation state. To do this, we took advantage of an epigenome editing tool recently validated by our group to over-express the histone monomethyltransferase *Setd7* to enrich for H3K4me1 (**Figure 6A**; Geiger, Balouek et al., 2024). AAV-*Setd7* broadly enriches for H3K4me1 without inducing further H3K4 methylation or other histone modifications associated with active gene expression (Geiger, Balouek et al., 2024). Thus, we predicted that global enrichment of H3K4me1 would induce or maintain open chromatin states similar to the epigenetic priming and H3K4me1 enrichment we observed after ELS (**Figure 3; Figure 4**).

Because ELS accelerated chromatin development, we over-expressed AAV-*Setd7* or AAV-*Gfp* in NAc at P10 to match the start of ELS (**Figure 6B**). Immunohistochemical staining showed successful targeting of the virus to the NAc even at this young age (**Figure 6C**). We used a within-subject design to test all male and female mice on behavioral tests both before and after sub-threshold adult social defeat stress (**Figure 6D-K**; Berton et al., 2006; Dias et al., 2014; Yohn et al., 2019; Balouek et al., 2023). We powered this study to detect sex differences. Notably, there were no main effects of sex on measures of social avoidance behavior, and thus males and females were analyzed together using a repeated-measures mixed effects model.

Both social defeat stress and epigenetic priming decreased social interaction time, a measure of threat avoidance [**Figure 6E, Supplemental Figure 4, Supplemental Table 4**; main effect of defeat: $F(1,56)=62.97$, $p<0.0001$; main effect of AAV-*Setd7*: $F(1,74)=4.63$, $p=0.034$; post-hoc comparison between GFP-Defeat and SETD7-Defeat with Benjamini FDR correction: $p=0.086$]. Similarly, both stress and AAV-*Setd7* decreased social interaction ratio [**Figure 6F**; main effect of defeat: $F(1,55)=23.86$, $p<0.0001$; main

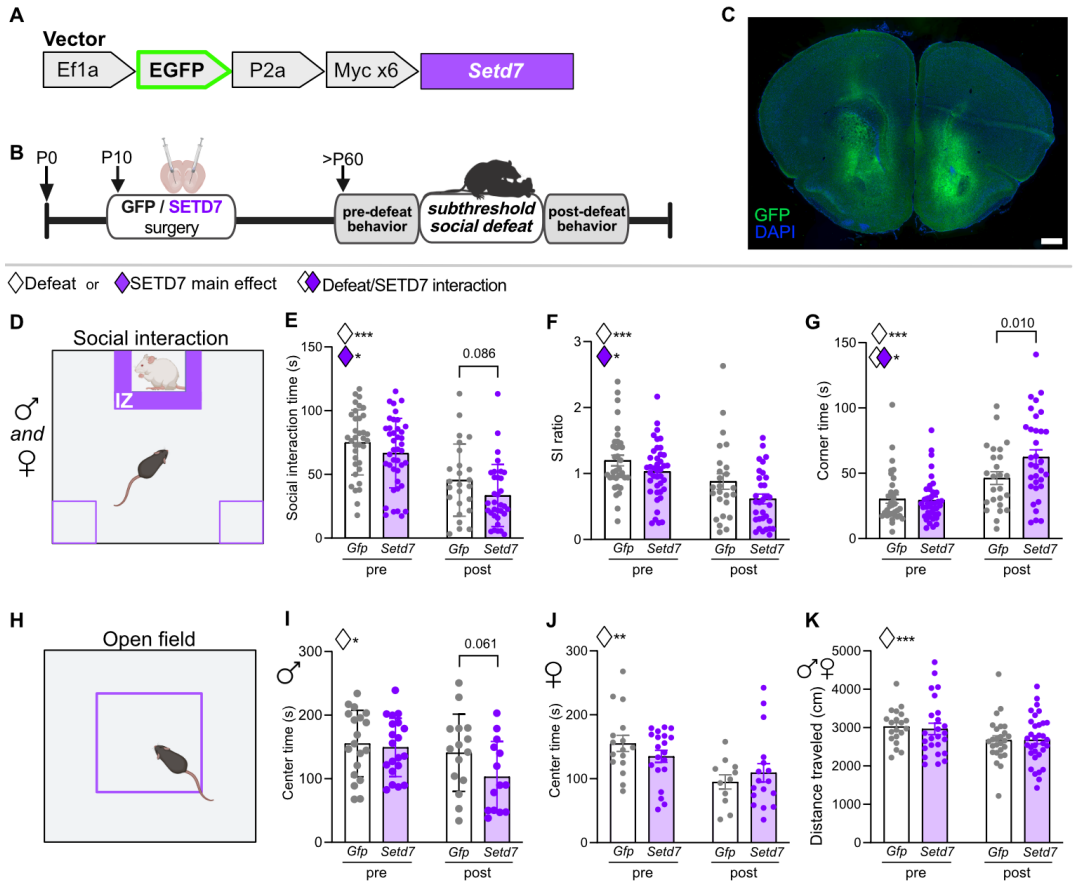

Figure 6 | Postnatal H3K4me1 enrichment in NAc increases sensitivity to future stress. **(A)** Experimental timeline. **(B)** Schematic of the *Setd7* over-expression vector packaged into AAVs; control vector was identical without *P2A-Myc-Setd7*. **(C)** Representative image showing viral targeting of NAc. Scale bar, 1mm. **(D)** Social interaction testing schematic: time spent in the interaction zone (IZ) or corners was measured. Within the social interaction test, **(E)** social interaction time, **(F)** social interaction ratio (lower ratio is associated with greater social avoidance), and **(G)** time spent in far corners among male and female mice before (pre) and after (post) social defeat. **(H)** Open field testing schematic. Within the open field test, time spent exploring the center among males **(I)** and females **(J)**. **(K)** Total distance traveled among males and females in the open field arena. Main effects of and interactions between *Setd7* and social defeat are denoted in the key (mean±SEM; *****p*<0.0001; ****p*<0.001; ***p*<0.01; **p*<0.05; *p*-values of post-hoc tests are shown).

effect of *Setd7*: F(1,74)=5.69, *p*=0.019]. Time spent huddling in corners, an additional measure of heightened vigilance and stress senitivity (Duque-Wilckens et al., 2020) was also increased in an interaction between stress and *Setd7* [**Figure 6G**; main effect of defeat: F(1,56)=45.9, *p*<0.0001; main effect of *Setd7*: F(1,73)=3.05, *p*=0.085; interaction between stress and *Setd7*: F(1,56)=5.94, *p*=0.018; post-hoc comparison between GFP-Defeat and SETD7-Defeat: *p*=0.010].

Time spent exploring the center of an open field, a more generalized measure of threat avoidance, was sensitive to stress, AAV-*Setd7*, and sex, and thus male and female mice were analyzed separately [trending three-way interaction between sex, stress, and *Setd7*: F(1,10=3.37), *p*=0.096]. Among males, both defeat and, to a lesser extent, *Setd7* decreased open field center time [**Figure 6I**; main effect of defeat: F(1,27)=6.26, *p*=0.019; main effect of *Setd7*: F(1,37)=2.49, *p*=0.123; post-hoc comparison between GFP-Defeat and SETD7-Defeat: *p*=0.061]. Among females, defeat but not *Setd7* decreased center time [**Figure 6J**; main effect of defeat: F(1,26)=14.67, *p*<0.001]. There was also a main effect of defeat on distance traveled among both males and females, but no effects of *Setd7*, indicating *Setd7* in the NAc did not impair mobility [**Figure 6K**; main effect of defeat: F(1,34)=15.20, *p*<0.001].

Taken together, this functional manipulation and behavioral results show that broad, developmental deposition of a histone modification associated with open chromatin mimics the effects of ELS to prime sensitivity to stress across the lifespan.

DISCUSSION

ELS sensitizes, or primes, individuals to subsequent stressors to increase lifetime risk of psychiatric disorders. At a cellular level, our recent work demonstrated that ensembles of neurons in the NAc that are active during ELS are preferentially reactivated by adult stress, which contributes to stress hypersensitivity and altered behavior (Balouek et al., 2023). At a molecular level, ELS programs both long-lasting baseline gene expression changes in the NAc and other afferent brain regions, and also primes gene expression response to a second hit of stress (Peña et al., 2019b; Kos et al., 2023). Here, we tested the hypothesis that ELS encodes these persistent changes in transcriptional reactivity within the NAc at an epigenetic level by priming cis-regulatory regions of the genome. Using a combination of activity-dependent cellular tagging, ATAC-sequencing across developmental time, bioinformatic analyses, viral-mediated epigenome editing, and behavioral quantification, we show that ELS initially opens chromatin in ELS-responsive cells — ultimately leading to chromatin remodeling throughout the NAc — and that deposition of a post-translational histone modification associated with open chromatin is sufficient to mimic ELS and prime hypersensitivity to future stress.

Enhancer priming — a form of molecular memory in which developmental or environmental cues open chromatin at enhancers and which is associated with presence of the post-translational histone modification H3K4me1 — facilitates a faster, stronger, and/or sensitized transcriptional response to recurring stimuli (Calo and Wysocka, 2013; D'Urso and Brickner, 2017; Lämke and Bäurle, 2017; Nord and West, 2020). This process is known to occur in botany, immunology, embryological development, and cancer (Cui et al., 2009; Bevington et al., 2016; Lämke and Bäurle, 2017; Vicente-Dueñas et al., 2018; Martin et al., 2021). Elegant work also demonstrated that experience can prime enhancers in the adult hippocampus through changes in 3D enhancer architecture, that priming is stable, and that memory recall activates enhancers (Marco et al., 2020). Our results reveal that ELS also leads to stable epigenetic priming. In the aftermath of ELS, we find that ELS largely opens chromatin (**Figure 2B**), that differentially accessible chromatin is enriched for enhancers and other cis-regulatory elements (**Figure 2E, Figure 3E**), and that ELS elevates H3K4me1 (**Figure 4D**). Through long-range interaction mapping to putatively contacted genes, we also show that ELS-opened regions, but not closed regions, predict the transcriptional response to a second hit of stress (**Figure 5B-C**). Furthermore, early developmental (P10) deposition of H3K4me1 in the NAc increases sensitivity to adult stress and alters behavior (**Figure 6**), demonstrating that epigenetic priming is functionally relevant and sufficient to recapitulate the effect of ELS at a behavioral level. Together, these data support an emerging role for enhancer priming as a biological mechanism for ELS-induced lifelong stress sensitivity.

While much effort has been made to characterize embryonic chromatin development (Gorkin et al., 2020), chromatin development in the brain between birth and adulthood has remained understudied. Recent research has demonstrated that the epigenetic landscape within cortical interneurons continues to mature postnatally and only crystalizes between mouse postnatal weeks 1 and 3, after which it is stable into adulthood (Stroud et al., 2020). This window of postnatal epigenetic maturation overlaps with the postnatal sensitive period for stress exposure in mice (Moriceau et al., 2010; Rincón-Cortés and Sullivan, 2014; Peña et al., 2017, 2019b, 2019a), suggesting that ELS may interfere with chromatin development. Indeed, we find that ELS accelerates maturation of chromatin in stress-responsive cells for both regions that typically open or close across development (**Figure 4B-C**). We also find that ELS accelerates and augments bulk levels of H3K4me1 (**Figure 4D**). ELS has similarly been found to accelerate other aspects of brain development, such as connectivity between amygdala and prefrontal cortical regions (Gee et al., 2013) and markers of hippocampal development including parvalbumin interneuron maturation, myelination, and synaptic plasticity (Bath et al., 2016). Accelerated development within some cell types or brain regions decouples otherwise tightly-controlled neurodevelopmental processes, which has been hypothesized to prematurely reduce plasticity and the ability to appropriately learn from expected environmental experiences (Reh et al., 2020; Rakesh et al., 2023). Our results show that these effects may arise from accelerated epigenetic development.

The finding that ELS initially opens chromatin in experience-responsive cells but ultimately leads to a more generalized chromatin response in the broader cell population — and not within experience-responsive cells — was unexpected. Profiling only tagged cells (as in some work, e.g. Marco et al., 2020) or a single time point would have precluded these findings. The lack of differences in chromatin accessibility in adult experience-responsive cells is reconciled by the finding that ELS accelerates standard maturation of chromatin within these cells, reflecting a change in timing of rather than overall chromatin opening (**Figure 4B-C**). However, several possibilities remain for our findings of delayed chromatin remodeling within initially non-activated cells. One possibility is that this epigenetic response is due to neurons initially activated by ELS remaining active and recruiting activation of surrounding neurons. However, we rejected this possibility given our earlier work showing that ELS leads neither to spontaneous neuronal reactivation of initially-responsive cells nor broader neuronal hyperactivity in the adult NAc in the absence of additional stress (Balouek et al., 2023). A second possibility is that this delayed epigenetic response reflects changes over time within the non-neuronal cell population. This hypothesis is supported by an enrichment of open chromatin in marker genes for oligodendrocytes, astrocytes, and microglia within non-activated cells after ELS (**Supplemental Figure 1**). Indeed, activation of neurons stimulates surrounding "peri-engram" astrocytes and other glia, which likely induces chromatin remodeling within these cells (Sun et al., 2024). Additionally, microglia adjacent to stress-responsive cells in the hypothalamus are disrupted by ELS and fail to prune excitatory synapses (Bolton et al., 2022). Neuronal activity also recruits surrounding microglia to aid in negative feedback of neuronal responses (Badimon et al., 2020), which may involve chromatin alterations to support changes in gene expression. This is an intriguing possibility because a lack of microglia-driven negative feedback also contributes to hyper-responsiveness of neurons to stimuli (Badimon et al., 2020), which could contribute to ELS-induced hyperresponsivity to stress. Further studies using spatially-resolved ATAC-seq are needed to determine whether adult chromatin alterations are greater among glial cells surrounding ELS-activated neurons.

In sum, these data provide novel evidence that ELS primes sensitivity to future stress though developmental changes in chromatin, akin to an epigenetic memory of stress within the NAc. Our research provides an important foundation for additional research to develop therapeutic strategies targeting chromatin to ameliorate the impact of ELS on brain development and psychiatric disease risk.

ACKNOWLEDGEMENTS

This research was funded by NIH R00MH115096 (CJP); NIH R01MH129643 (CJP); NIH F31 MH131351 (RR); and the New York Stem Cell Foundation (CJP). CJP is a New York Stem Cell Foundation Robertson Investigator. We would like to thank Hope Kronman for sharing the raw NAc MS data from (Kronman et al., 2021), Julie-Anne Balouek for initially generating the *Setd7* over-expression virus and for project consultation (Geiger, Balouek et al., 2024), and Ricardo Mallarino for manuscript input. We would also like to thank Wei Wang and the Genomics Core Facility in the Lewis-Sigler Institute for Integrative Genomics at Princeton (LSI) where ATAC-seq was performed, as well as Lance Parsons at LSI for his input and help constructing ATAC-seq analytical workflows. Parts of some figures were generated with BioRender.com.

AUTHOR CONTRIBUTIONS

These studies were designed by CJP and RLR. ATAC-seq data were collected by RLR and analyzed by RLR, MD, NA, OMO, and CJP; immunohistochemistry data were collected by HJJK; mouse work was performed by RLR, LWH, HJJK, and SNB. The manuscript was written by RLR, CJP, and MD with input from all authors.

COMPETING INTERESTS

There are no conflicts of interest to report.

METHODS

Mice

All experiments were conducted in accordance with the guidelines of the Institutional Animal Care and Use Committee at Princeton University. Mice were housed in a temperature- and humidity-controlled vivarium and maintained on a 12-h light/dark cycle (lights on at 4a.m.) and were group-housed in sets of three to five with *ad libitum* access to food and water. Mice were considered to be "male" or "female" based on external genitalia (adult) and/ or anogenital distance (pups). For all experiments, mice were bred in-house in trios, males were removed after 5-7 days, and females were separated into individual cages 1-3 days prior to parturition. All offspring regardless of early life experience were weaned at postnatal day P21, with males and females weaned into separate cages, keeping littermates together and only combining pups from different litters of the same experimental condition in order to maintain at least three mice/cage. Males and females were used in all experiments.

In order to tag and isolate experience-responsive cells for ATAC-seq experiments, we generated Arc-CreER^{T2} X Sun1-GFP double-transgenic mice on a C57BL/6J background as previously described (Balouek et al., 2023). Briefly, heterozygous Arc-CreERT$^{2/+}$ mice (stock #022357, The Jackson Laboratory; (Denny et al., 2014) were bred in-house with R26-CAG-LSL-Sun1-sfGFP-Myc knock-in mice ("Sun1-GFP"; stock #030952, The Jackson Laboratory; (Mo et al., 2015). Genotyping of double-transgenic mice was performed as previously described (Balouek et al., 2023).

Wild-type C57BL/6J mice were bred in-house and used for viral-mediated gene manipulation and behavior experiments. Retired Swiss-Webster male breeder mice (Taconic) were housed individually and used as aggressor mice in social defeat stress.

Administration of 4-hydroxytamoxifen

To induce experience-dependent recombination, 4-hydroxytamoxifen (4-OHT) was administered as described (Balouek et al., 2023). 4-OHT (catalog #H7904, Sigma-Aldrich) was first prepared as 25mg/ml stock solutions in ethanol and frozen at -20°C. For injections, 4-OHT was prepared fresh daily from stock to 5mg/ml, dissolved in ethanol and corn oil (1:4). Double-transgenic Arc-CreER^{T2} X Sun1-GFP pups were first habituated to injections of saline (60 µL i.p.) from P14-16. To drive recombination on P17, (the last day of the stress for ELS pups), transgenic pups were injected with 4-OHT (50 mg/kg body weight, approximately 60 µL/pup, i.p.) at the beginning of maternal separation. Standard-reared pups were returned to their home cage and given a novel enrichment object (running wheel: pups were observed to explore the novel object but not necessarily run on it) in order to tag a specific positive-valence experience. The mice were then left undisturbed for at least three days (P17-P21) to allow time for expression of the transgenes to develop before collecting tissue and isolating nuclei. We previously validated the use of these mice for experience-specific tagging, and showed that we were able to tag similar numbers of neurons in ELS and Std NAc so as not to artificially bias downstream analyses.

Stress paradigms

Early-life stress (ELS): Litters for ATAC-seq were randomly assigned at birth to standard (Std)-rearing or ELS

conditions. The ELS paradigm used was a combination of maternal separation and limited nesting resources during a stress sensitive period from postnatal day P10-17, based on established protocols (Peña et al., 2017). Briefly, pups in ELS-assigned litters were separated from their dams together into a clean cage containing a tablespoon of bedding from an adult male aggressor mouse for 3-4 h/day from P10-17. During the week of daily separations, home cage nesting material was also reduced to 1/2 of a nesting puck, which was replaced with a full nesting puck after the last day of stress.

Adult sub-threshold social defeat stress: In order to determine whether chromatin manipulation increased sensitivity to later stress, male and female mice were subject to sub-threshold adult social defeat stress for 5 consecutive days. Previous studies have found that among control males, susceptibility to chronic social defeat stress develops across 10 days, but is not apparent after only 5 (Dias et al., 2014; Hodes et al., 2015; Muir et al., 2020). Here, both male and female mice were exposed to social defeat but were run in separate cohorts. Males were defeated as described in standard protocols (Golden et al., 2011). Females were defeated in a "non-discriminatory" version of social defeat as previously described (Yohn et al., 2019; Bennett et al., 2024; Geiger, Balouek et al., 2024). Briefly, on each day of social defeat, experimental mice were placed into the cage of a novel Swiss-Webster retired breeder ("aggressor"; Taconic) mouse. Male lures were introduced first for ~1-2 minutes, then an experimental female mouse was added into the cage for an additional 5 minutes. After defeat, mice were moved across a perforated plexiglass barrier for the remainder of the day for continued sensory contact. Experimental mice were introduced to a new aggressor each day. Control mice were housed in a standard mouse cage in pairs of the same sex, separated by a perforated plexiglass barrier. Behavioral testing began one day after the last bout of social defeat.

Stereotaxic surgery

Standard-reared male and female C57BL/6J pups were randomly assigned to either experimental *Setd7* over-expression group or a control *Gfp* group and surgeries were performed as previously described (Geiger, Balouek et al., 2024) with the exception of NAc-targeting surgical coordinates. P9-12 pups were anesthetized with isoflurane (2-3% induction; 1-3% maintenance) for surgeries and fitted into dual-arm stereotax with the nose fitted in the nose cone above the bite bar and the head stabilized using blunt ends of ear bars between the jaw and ear. Pups were bilaterally administered either AAV-GFP (AAV-EF1a-EGFP) or AAV-SETD7 (AAV-EF1a-EGFP-P2A-MYC-Setd7) into the nucleus accumbens. The surgical coordinates were +/- 1.4 (x = medial/lateral plane), +1.0(y = anterior/posterior plane), -3.15(z = dorsal/ventral plane), with both Hamilton syringes angled at 7˚. 250nL of virus was administered into each hemisphere at a rate of 0.1μL/minute. Both vet glue (Covetrus, cat#: 001505) and two-four sterile sutures (Fisher, cat#: 501180710) were used to ensure complete healing of incisions. Mice were given a perioperative topical dose of bupivacaine (0.25%, 2 mg/kg) and an additional dose 24h following surgery. Mice recovered in a partially-warmed cage before being returned to their home cage. To prevent cannibalization of pups by dams following surgery, pups were only returned to the home cage with the dam once completely ambulatory. Mice were given an additional topical dose of bupivacaine 24h following surgery, monitored for five days, weaned at P21, and aged to adulthood in standard group housing conditions.

Behavioral paradigms and analysis

Mice were tested on a set of two behavioral tests twice for within-subject controls: once prior to ("pre") and once after social defeat stress ("post"). Groups are presented as GFP-control (AAV-*Gfp*, no social defeat stress), GFP-defeat (AAV-*Gfp*, social defeat stress), SETD7-control (AAV-*Setd7* virus, no social defeat stress), SETD7-defeat (AAV-*Setd7*, social defeat stress). Social interaction and open field exploration testing were performed as previously described (Peña et al., 2017; Balouek et al., 2023; Bennett et al., 2024). All behavior was recorded and initially analyzed with Ethovision software.

Social interaction: To assess social avoidance behavior, experimental mice were tested in a two-stage social interaction test. In the first 2.5-minute stage, experimental mice were placed into a novel empty arena (44 x 44 x 20 cm) with an empty enclosure along one wall. Mice were then removed, a novel aggressor mouse was placed into the enclosure in the "social interaction zone," and experimental mice were reintroduced into the arena for an additional 2.5 minutes. Time spent in the interaction zones and in the corners was measured. Social interaction ratio was calculated as time spent in the interaction zone with the aggressor present divided by time spent in the interaction zone without the aggressor present.

Open field: Each mouse was allowed to explore an empty arena (44 x 44 x 20 cm) for 10 minutes and time spent in the center of the arena and overall distance traveled were measured.

Statistical analysis: Behavioral data were graphed and analyzed using Graphpad PRISM software (v. 10.0.3). Outliers were considered to be >2 standard-deviations away from group mean and were removed to avoid type-II error. Main effects and interactions between viral manipulation and social defeat were determined by mixed effects model to account for within-subject repeated testing, with Sidak's multiple comparisons testing for *post hoc* pairwise analysis. All significance thresholds were set at $p<0.05$; trends were reported for $p<0.1$.

Nuclear isolation and ATAC-sequencing

Double-transgenic Arc-CreER^{T2} X Sun1-GFP mice allowed for affinity purification of nuclei expressing the SUN1-GFP-MYC fusion protein in the nuclear membrane by the INTACT approach (Deal and Henikoff, 2010; Mo et al., 2015). Brains were harvested from mice after cervical dislocation and rapid decapitation into ice-cold homogenization buffer at either P21 (juvenile time point, three days after recombination) or in adulthood (P60-90). Tissue was used immediately or flash-frozen until use. To isolate nuclei, 14-gauge bilateral punches of the NAc were made on 1mm slices of brain tissue and dounce homogenized in 1.5mL of 1X Unstable homogenization buffer (Corces et al., 2017). Homogenate was transferred to 2mL lo-bind tubes then spun down at 500 x g for 5 min (at 4C). Nuclei were collected by iodixanol gradient and counts were collected using a hemocytometer. Nuclei from tagged cells were separated from non-tagged nuclei by incubation with anti-GFP (Sigma; cat#SAB4301138-100UL) and anti-myc (Sigma; cat#: SAB4300318-100UG) antibodies that bound to magnetic Protein G Dynabeads (ThermoFisher; cat#10004D). Total yield of nuclei for all samples was ~600k nuclei, and activated nuclei made up ~10% of the total yield. Both populations of cells were kept and immediately used for ATAC-sequencing. All reactions were performed on ice.

Nuclei from activated and non-activated cells were transposed using Illumina's transposition kit (Illumina; cat#20034198) for 35 minutes for non-activated and 40 minutes for activated nuclei at 37°C at 1000RPM. Fragmented DNA was recovered with Qiagen MinElute kits (Qiagen; cat# 28604). Samples were amplified and purified according to Corces et al. (2017) using Illumina UD indexes (Illumina; cat#20027214 A or B) and AMPure XP beads (ThermoFisher; cat#NC9959336). Resulting yield of DNA fragment sizes was determined by Bioanalyzer dsDNA High Sensitivity protocol and normalized by concentration for sequencing.

Experience-activated samples: Juvenile samples included 5 Std and 6 ELS samples (ELS: 3 male and 3 female samples, Std-activated: 2 male and 3 female samples) harvested from two different cohorts. Samples from the first cohort (two per group) included pooled bilateral NAc tissue punches from two mice per sample, while samples from the second cohort (3 Std and 4 ELS) were from individual mice. Adult samples included 3 Std and 3 ELS samples (ELS: 2 male and 1 female samples, Std: 1 male and 2 female samples) and were from individual mice.

Non-activated samples: Juvenile samples included 7 Std and 7 ELS samples (ELS: 4 male and 3 female samples, Std-activated: 4 male and 3 female samples). Adult samples included 3 Std and 2 ELS samples (ELS: 1 male and 1 female samples, Std: 1 male and 2 female samples). All samples were from individual mice.

Sequencing and statistical analysis

All samples were sequenced within the Genomics Core Facility of the Lewis-Sigler Institute at Princeton University on a NovaSeq using S1 100nt chemistry to yield ~1.3-1.6 B read depth (adult time point and juvenile cohort 2). NovaSeq using SP 100nt chemistry to yield ~325-400M read depth was used for juvenile cohort 1. FASTQ quality controls were used to show quality of reads on average (>30 Phred) for all samples, and only samples with a Phred score >30 were used. Alignment was performed to mm10 (/grcm38) genome by Bowtie2 and low quality or duplicate reads were filtered out. Libraries were normalized and adjusted for differences in read depth. Broad peaks were defined using MACS2, with a *q*-value cutoff of 0.05. Consensus peaksets were created with bedtools. featurecounts was used to create single count matrices for use in differential analysis. Differential analysis was performed using edgeR with TMM normalization to allow for comparisons between samples, and low count regions (less than 2 CPM in at least 8 samples in each neuronal activation class) were removed.

Cell-type analysis

To estimate cell type composition, we quantified rpm/cpm-normalized ATAC-seq reads within 500 bp of any annotated TSS (GENCODE VM23) for each marker gene *(Drd1*, *Drd2, Drd3, Pdyn, Grm8, Chat, Pvalb, Mog, Aqp4, Cxcr1)*. Normalization and quantification was performed using the R/Bioconductor package BRGenomics (v1.13.0; DeBerardine 2024; 10.18129/B9.bioc.BRGenomics; (DeBerardine, 2023) and boxplots were generated using ggplot2 (v3.4.4). Visualizations of tracks for these genes were generated using the WashU epigenome browser (https://epigenomegateway.wustl.edu/browser/) using rpm/cpm-normalized bigWig files.

Bioinformatic analysis: genomic features, motif analysis, contacted gene prediction, looping visualizations, and gene ontology analysis

To determine which genomic features differentially accessible regions (DARs) belonged to, the Bioconductor package GenomicDistributions(1.8.0) was used. The mm10 package was loaded and enhancers were added to the list of features (partitionList from November 2020 ENSEMBL build [https://nov2020.archive.ensembl.org/]).

Motif Analysis was carried out using XTREME, of the MEME suite (https://meme-suite.org/meme/tools/xstreme) (Grant and Bailey, 2021). Significantly upregulated and downregulated regions were supplied to the motif discovery pipeline, using the HOCOMOCO Mouse v11 FULL parameter for known motifs. All other parameters were kept at default; an *E* value of ≤ 0.05 was used as a significance threshold, and motifs were only reported if they appeared in >60% of input regions*. (*Except for ERR2/RARA and FOXJ

in the activated juvenile condition, which were each present in 55% of input regions, and IRF3 in the adult non-activated population, in which 40% and 20% of open DAR regions had respectively 1 or 2 IRF3 motifs.)

In order to identify genes putatively contacted and regulated by DARs, we used the T-Gene tool within MEME-suite (O'Connor et al., 2020). We first lifted-over our ATAC-seq peaks from mm10 to mm9 using a chain file downloaded from the UCSC genome browser (http://hgdownload.cse.ucsc.edu/goldenpath/mm10/liftOver/mm10ToMm9.over.chain.gz) and the re-implementation of UCSC liftOver found in the R/Bioconductor package rtracklayer (v1.58.0). During liftOver, peaks that failed to lift over, or lifted over into multiple non-contiguous peaks, were dropped from this analysis (n=0 for adultBB_open_annotations.bed; n=1 for adultBB_closed_annotations.bed and juvBB_closed_annotations.bed; and n=3 for juvBB_open_annotations.bed). Regions that survived the lift over were then used in T-Gene. Output of T-Gene is limited to 1000 putative gene contacts. We applied a cutoff of $p<0.1$ to identify the strongest contact predictions. We visualized contacts between regions of open chromatin and potential-contacted genes using the WashU Epigenome Browser (http://epigenomegateway.wustl.edu/)(Li et al., 2019) with mm10 Brain Tracks from the 4D Nucleome Network, in Arc mode (Reiff et al., 2022). Potential chromatin contacts are shown with ATAC-seq tracks as indicated. Publicly available and pre-loaded brain Hi-C data was used for looping visualizations between gene promoters and putative regulatory elements. Hi-C data was collected from the dataset (https://data.4dnucleome.org/experiment-set-replicates/4DNESRWDFFF8/), from (Deng et al., 2015).

Gene Ontology (GO) biological process terms were generated using the DOSE R package for genes most likely contacted by open and closed regions and plotted by –log10(adjusted p-value).

Gene expression predictions

In order to predict the impact of changes in chromatin accessibility on gene expression response to adult stress, we filtered lists of genes putatively-contacted by DARs to only those consistently associated with open or consistently associated with closed chromatin at both juvenile and adult time points. We then used previously published RNA-seq from adult NAc to determine how the expression of these genes changed from Std-Control conditions with ELS, Social Defeat, or ELS+Defeat (Peña et al., 2019b); GEO GSE89692; differential expression calculated by DEseq2). Genes with expression <5 CPM were excluded. We visualized the $\log_2$Fold-Change of these expression changes using Morpheus (https://software.broadinstitute.org/morpheus) with rows transformed by subtracting row mean and dividing by row standard deviation. Hierarchical clustering was then performed on the gene rows. We calculated a "RNA predictive factor" as [L2FC * (1-*p*-value)] such that stronger statistical significance and greater fold-change would be more heavily weighted, and that positive L2FC values (corresponding to increases in gene expression as would be predicted from open chromatin at gene regulatory regions) would produce positive predictive factors, and negative L2FC (corresponding to decreases in gene expression, opposite to open chromatin predictions) would produce negative predictive factors. For RNA predictive factors for closed regions, [-L2FC * (1-*p*-value)] was used so that more positive values always indicated higher predictive value, assuming closed chromatin would predict decreased gene expression. Predictive factors were then averaged across all genes for each group. Analysis of group differences was performed by two-tailed one-sample t-test with a null of 0 (no predictive value) and alpha=0.05.

Linear mixed effects analysis for chromatin development

A linear mixed effects model was used to allow both fixed and random effects given multiple levels of variability in the data (i.e., ELS, sex, and age) and non-independence among the chromatin regions (i.e. each individual sample contributed multiple open chromatin regions), using the LME function in R. Normalized counts represent the relative accessibility of chromatin. Individual samples were taken as random effects in this hierarchical model to examine the significance and interaction effects of stress and age, stress and sex, and the individual fixed effects. Beta estimates, standard-error, and *p*-values are reported.

Histone modification analysis

Analysis of post-translational histone modifications in NAc across three developmental time points (P21, P35, P70-90, n=3 males/group/age) was done by re-analyzing previously published histone post-translational modification mass spectrometry (data from (Kronman et al., 2021). This data represents percentage of each measured histone modification per fragmented histone peptide (for example, percentage of unmodified histone-3 lysine-4, H3K4me1, H3K4me2, and H3K4me3). Data for H3K27me2 and H3K27me3 are summations of the modification of interest alone or in combination with any H3K36 modification measured on the same peptide fragment. For each histone modification of interest, two-way ANOVA was done to assess main effects and interactions of ELS with age, followed by post-hoc testing with Sidak's multiple comparisons correction to assess impact of ELS at each age. Alpha=0.05.

Immunohistochemistry and imaging

To confirm viral targeting of the NAc, following behavior testing, a subset of mice was anesthetized by i.p. injection of 100 mg/kg ketamine and 10 mg/kg xylazine, then euthanized and transcardially perfused with ice-cold

saline followed by 4% paraformaldehyde (PFA). Brains were dissected and submerged in fresh 4% PFA at 4°C overnight, then stored in 30% sucrose solution for an additional 2 days (until the tissue became isotonic). Dry ice was used to flash-freeze the brains, after which they were kept at -80°C until slicing. For slicing, the frozen brains were embedded in Tissue-Plus™ O.C.T. Compound (Fisher Scientific) to maintain structural integrity. A cryostat held at -20°C was used to slice the brains at 20µm. Brain slices were mounted directly onto Superfrost™ Plus microscope slides (Fisher Scientific) and stored at -20°C ahead immunohistochemical staining.

Immunohistochemistry entailed the following steps (at room temperatures unless noted): (1) Rinsing the slices in 1 X phosphate-buffered saline (PBS) 3 times for 5 min each. (2) Incubating the slices in 1.5% normal donkey serum (NSD) in 1 X PBS-Triton X-100 solution for 1 h. (3) Incubating the slices in primary antibody [1:500 Anti-Green Fluorescent Protein (Chicken) Antibody (Aves Labs); 1:150 SETD7 Mouse Monoclonal Antibody (OriGene); and 1.5% NSD in 1 X PBS-Triton X-100 solution] overnight at 4°C. (4) Rinsing the slices in 1 X PBS 3 times for 5 min each. (5) Incubating the slices in a secondary antibody solution [1:500 Alexa Fluor® 488 AffiniPure Donkey Anti-Chicken IgY (IgG) (H+L) (Jackson ImmunoReseach Labs); 1:500 Cy™3 AffiniPure Donkey Anti-Mouse IgG (H+L) (Jackson ImmunoReseach Labs); and 1.5% NSD in 1 X PBS-Triton X-100] for 1 h. (6) Rinsing the slices in 1 X PBS 3 times for 5 min each. (7) Incubating the slices in 0.0025% DAPI solution for 5 min. (8) Rinsing the slices in 1 X PBS 3 times for 5 min each. Following the last rinse, Fluoromount-G® mounting media (SouthernBiotech) was used to coverslip the immune-stained slices. Samples were kept at 4°C until imaging. Fluorescent imaging was performed with a Nanozoomer S60 slide scanner (Hamamatsu). All images were processed using the ImageJ (version 1.2.0) software containing the FIJI plugin (NIH, Bethesda, MD, USA).

Data Availability: All sequencing data will be deposited in NCBI's Gene Expression Omnibus. All other data will be made available upon reasonable request.

SUPPLEMENTAL MATERIAL

Supplemental Figure 1: Cell-type estimation in experience-activated and non-activated cell populations

Supplemental Figure 2: Postnatal development of chromatin in initially non-activated cell populations

Supplemental Figure 3: Post-translational histone modifications across development

Supplemental Figure 4: Example heatmaps of social interaction behavior after social defeat

Supplemental Table 1: ATAC-seq reads and mapping rates

Supplemental Table 2: Linear mixed effects model statistics for the impact of ELS on chromatin development

Supplemental Table 3: Overlapping gene lists

Supplemental Table 4: Behavioral testing statistics

REFERENCES

Ana Maria, A., Oscar Andréas, M.-R., & Haider, N. B. (2015). Role of Nuclear Receptors in Central Nervous System Development and Associated Diseases. *Journal of Experimental Neuroscience*, *9s2*, JEN.S25480. https://doi.org/10.4137/JEN.S25480

Badimon, A., Strasburger, H. J., Ayata, P., Chen, X., Nair, A., Ikegami, A., Hwang, P., Chan, A. T., Graves, S. M., Uweru, J. O., Ledderose, C., Kutlu, M. G., Wheeler, M. A., Kahan, A., Ishikawa, M., Wang, Y.-C., Loh, Y.-H. E., Jiang, J. X., Surmeier, D. J., … Schaefer, A. (2020). Negative feedback control of neuronal activity by microglia. *Nature*, 1–7. https://doi.org/10.1038/s41586-020-2777-8

Bading, H., Segal, M. M., Sucher, N. J., Dudek, H., Lipton, S. A., & Greenberg, M. E. (1995). *N*-methyl-d-aspartate receptors are critical for mediating the effects of glutamate on intracellular calcium concentration and immediate early gene expression in cultured hippocampal neurons. *Neuroscience*, *64*(3), 653–664. https://doi.org/10.1016/0306-4522(94)00462-E

Balouek, J.-A., Mclain, C. A., Minerva, A. R., Rashford, R. L., Bennett, S. N., Rogers, F. D., & Peña, C. J. (2023). Reactivation of Early-Life Stress-Sensitive Neuronal Ensembles Contributes to Lifelong Stress Hypersensitivity. *Journal of Neuroscience*, *43*(34), 5996–6009. https://doi.org/10.1523/JNEUROSCI.0016-23.2023

Bath, K. G., Manzano-Nieves, G., & Goodwill, H. (2016). Early life stress accelerates behavioral and neural maturation of the hippocampus in male mice. *Hormones and Behavior*, *82*, 64–71. https://doi.org/10.1016/j.yhbeh.2016.04.010

Bennett, S. N., Chang, A. B., Rogers, F. D., Jones, P., & Peña, C. J. (2024). Thyroid hormones mediate the impact of early-life stress on ventral tegmental area gene expression and behavior. *Hormones and Behavior*, *159*, 105472. https://doi.org/10.1016/j.yhbeh.2023.105472

Berton, O., Mcclung, C. A., Dileone, R. J., Krishnan, V., Renthal, W., Russo, S. J., Graham, D., Tsankova, N. M., Bolaños, C. A., Rios, M., Monteggia, L. M., Self, D. W., & Nestler, E. J. (2006). Essential role of BDNF in the mesolimbic dopamine pathway in social defeat stress. *Science*, *311*(5762), 864–868. https://doi.org/10.1126/science.1120972

Bevington, S. L., Cauchy, P., Piper, J., Bertrand, E., Lalli, N., Jarvis, R. C., Gilding, L. N., Ott, S., Bonifer, C., & Cockerill, P. N. (2016). Inducible chromatin priming is associated with the establishment of immunological memory in T cells. *The EMBO Journal*, *35*(5), 515–535. https://doi.org/10.15252/embj.201592534

Bolton, J. L., Short, A. K., Othy, S., Kooiker, C. L., Shao, M., Gunn, B. G., Beck, J., Bai, X., Law, S. M., Savage, J. C., Lambert, J. J.,

Belelli, D., Tremblay, M.-È., Cahalan, M. D., & Baram, T. Z. (2022). Early stress-induced impaired microglial pruning of excitatory synapses on immature CRH-expressing neurons provokes aberrant adult stress responses. *Cell Reports*, *38*(13), 110600. https://doi.org/10.1016/j.celrep.2022.110600

Buenrostro, J. D., Giresi, P. G., Zaba, L. C., Chang, H. Y., & Greenleaf, W. J. (2013). Transposition of native chromatin for fast and sensitive epigenomic profiling of open chromatin, DNA-binding proteins and nucleosome position. *Nature Methods*, *10*(12), 1213–1218. https://doi.org/10.1038/nmeth.2688

Calo, E., & Wysocka, J. (2013). Modification of Enhancer Chromatin: What, How, and Why? *Molecular Cell*, *49*(5), 825–837. https://doi.org/10.1016/j.molcel.2013.01.038

Corces, M. R., Trevino, A. E., Hamilton, E. G., Greenside, P. G., Sinnott-Armstrong, N. A., Vesuna, S., Satpathy, A. T., Rubin, A. J., Montine, K. S., Wu, B., Kathiria, A., Cho, S. W., Mumbach, M. R., Carter, A. C., Kasowski, M., Orloff, L. A., Risca, V. I., Kundaje, A., Khavari, P. A., … Chang, H. Y. (2017). An improved ATAC-seq protocol reduces background and enables interrogation of frozen tissues. *Nature Methods*, *14*(10), Article 10. https://doi.org/10.1038/nmeth.4396

Cui, K., Zang, C., Roh, T.-Y., Schones, D. E., Childs, R. W., Peng, W., & Zhao, K. (2009). Chromatin signatures in multipotent human hematopoietic stem cells indicate the fate of bivalent genes during differentiation. *Cell Stem Cell*, *4*(1), 80–93. https://doi.org/10.1016/j.stem.2008.11.011

Deal, R. B., & Henikoff, S. (2010). A Simple Method for Gene Expression and Chromatin Profiling of Individual Cell Types within a Tissue. *Developmental Cell*, *18*(6), 1030–1040. https://doi.org/10.1016/j.devcel.2010.05.013

DeBerardine, M. (2023). BRGenomics for analyzing high-resolution genomics data in R. *Bioinformatics*, *39*(6), btad331. https://doi.org/10.1093/bioinformatics/btad331

Deng, X., Ma, W., Ramani, V., Hill, A., Yang, F., Ay, F., Berletch, J. B., Blau, C. A., Shendure, J., Duan, Z., Noble, W. S., & Disteche, C. M. (2015). Bipartite structure of the inactive mouse X chromosome. *Genome Biology*, *16*(1), 152. https://doi.org/10.1186/s13059-015-0728-8

Denny, C. A., Kheirbek, M. A., Alba, E. L., Tanaka, K. F., Brachman, R. A., Laughman, K. B., Tomm, N. K., Turi, G. F., Losonczy, A., & Hen, R. (2014). Hippocampal memory traces are differentially modulated by experience, time, and adult neurogenesis. *Neuron*, *83*(1), 189–201. https://doi.org/10.1016/j.neuron.2014.05.018

Dias, C., Feng, J., Sun, H., Shao, N. yi, Mazei-Robison, M. S., Damez-Werno, D., Scobie, K., Bagot, R., Labonté, B., Ribeiro, E., Liu, X., Kennedy, P., Vialou, V., Ferguson, D., Peña, C., Calipari, E. S., Koo, J. W., Mouzon, E., Ghose, S., … Nestler, E. J. (2014). β-catenin mediates stress resilience through Dicer1/microRNA regulation. *Nature*, *516*(7529), 51–55. https://doi.org/10.1038/nature13976

Duque-Wilckens, N., Torres, L. Y., Yokoyama, S., Minie, V. A., Tran, A. M., Petkova, S. P., Hao, R., Ramos-Maciel, S., Rios, R. A., Jackson, K., Flores-Ramirez, F. J., Garcia-Carachure, I., Pesavento, P. A., Iñiguez, S. D., Grinevich, V., & Trainor, B. C. (2020). Extrahypothalamic oxytocin neurons drive stress-induced social vigilance and avoidance. *Proceedings of the National Academy of Sciences*, 202011890. https://doi.org/10.1073/pnas.2011890117

D'Urso, A., & Brickner, J. H. (2017). Epigenetic transcriptional memory. *Current Genetics*, *63*(3), 435–439. https://doi.org/10.1007/s00294-016-0661-8

Ferrari, K. J., Scelfo, A., Jammula, S., Cuomo, A., Barozzi, I., Stützer, A., Fischle, W., Bonaldi, T., & Pasini, D. (2014). Polycomb-Dependent H3K27me1 and H3K27me2 Regulate Active Transcription and Enhancer Fidelity. *Molecular Cell*, *53*(1), 49–62. https://doi.org/10.1016/j.molcel.2013.10.030

Francis, T. C., Chandra, R., Friend, D. M., Finkel, E., Dayrit, G., Miranda, J., Brooks, J. M., Iñiguez, S. D., O'Donnell, P., Kravitz, A., & Lobo, M. K. (2014). Nucleus Accumbens Medium Spiny Neuron Subtypes Mediate Depression-Related Outcomes to Social Defeat Stress. *Biological Psychiatry*. https://doi.org/10.1016/j.biopsych.2014.07.021

Gallia, G. L., Johnson, E. M., & Khalili, K. (2000). SURVEY AND SUMMARY: Purα: a multifunctional single-stranded DNA- and RNA-binding protein. *Nucleic Acids Research*, *28*(17), 3197–3205. https://doi.org/10.1093/nar/28.17.3197

Gee, D., Gabard-Durnam, L. J., Flannery, J., Goff, B., Humphreys, K. L., Telzer, E. H., Hare, T. A., Bookheimer, S. Y., & Tottenham, N. (2013). Early developmental emergence of human amygdala–prefrontal connectivity after maternal deprivation. *Proceedings of the National Academy of Sciences of the United States of America*, *110*(39), 15638–15643. https://doi.org/10.1073/pnas.1307893110

Geiger, L. T., Balouek, J.-A. R., Farrelly, L. A., Chen, A. S., Tang, M., Bennett, S. N., Nestler, E. J., Garcia, B. A., Maze, I., & Peña, C. J. (2024). Early-life stress alters chromatin modifications in VTA to prime stress sensitivity. *bioRxiv*. https://doi.org/10.1101/2024.03.14.584631

Giano, Z., Wheeler, D. L., & Hubach, R. D. (2020). The frequencies and disparities of adverse childhood experiences in the U.S. *BMC Public Health*, *20*(1), 1327. https://doi.org/10.1186/s12889-020-09411-z

Godino, A., Salery, M., Cuttoli, R. D., Estill, M. S., Holt, L. M., Futamura, R., Browne, C. J., Mews, P., Hamilton, P. J., Neve, R. L., Shen, L., Russo, S. J., & Nestler, E. J. (2023). Transcriptional control of nucleus accumbens neuronal excitability by retinoid X receptor alpha tunes sensitivity to drug rewards. *Neuron*, *0*(0). https://doi.org/10.1016/j.neuron.2023.02.013

Golden, S. A., Covington, H. E., Berton, O., & Russo, S. J. (2011). A standardized protocol for repeated social defeat stress in mice. *Nature Protocols*, *6*(8), 1183–1191. https://doi.org/10.1038/nprot.2011.361

Gorkin, D. U., Barozzi, I., Zhao, Y., Zhang, Y., Huang, H., Lee, A. Y., Li, B., Chiou, J., Wildberg, A., Ding, B., Zhang, B., Wang, M., Strattan, J. S., Davidson, J. M., Qiu, Y., Afzal, V., Akiyama, J. A., Plajzer-Frick, I., Novak, C. S., … Ren, B. (2020). An atlas of dynamic chromatin landscapes in mouse fetal development. *Nature*, *583*(7818), Article 7818. https://doi.org/10.1038/s41586-020-2093-3

Grant, C. E., & Bailey, T. L. (2021). *XSTREME:*

Comprehensive motif analysis of biological sequence datasets (p. 2021.09.02.458722). bioRxiv. https://doi.org/10.1101/2021.09.02.458722

Green, J. G., McLaughlin, K. A., Berglund, P. A., Gruber, M. J., Sampson, N. A., Zaslavsky, A. M., & Kessler, R. C. (2010). Childhood Adversities and Adult Psychiatric Disorders in the National Comorbidity Survey Replication I: Associations With First Onset of DSM-IV Disorders. *Archives of General Psychiatry*, *67*(2), 113–123. https://doi.org/10.1001/archgenpsychiatry.2009.186

Hackman, D. A., Farah, M. J., & Meaney, M. J. (2010). Socioeconomic status and the brain: Mechanistic insights from human and animal research. *Nature Reviews Neuroscience*, *11*(9), 651–659. https://doi.org/10.1038/nrn2897

Hannenhalli, S., & Kaestner, K. H. (2009). The evolution of Fox genes and their role in development and disease. *Nature Reviews Genetics*, *10*(4), 233–240. https://doi.org/10.1038/nrg2523

Hanson, J. L., Albert, D., Iselin, A.-M. R., Carré, J. M., Dodge, K. A., & Hariri, A. R. (2016). Cumulative stress in childhood is associated with blunted reward-related brain activity in adulthood. *Social Cognitive and Affective Neuroscience*, *11*(3), 405–412. https://doi.org/10.1093/scan/nsv124

Hanson, J. L., Hariri, A. R., & Williamson, D. E. (2015). Blunted Ventral Striatum Development in Adolescence Reflects Emotional Neglect and Predicts Depressive Symptoms. *BPS*, *78*(9), 598–605. https://doi.org/10.1016/j.biopsych.2015.05.010

Hanson, J. L., Knodt, A. R., Brigidi, B. D., & Hariri, A. R. (2018). Heightened connectivity between the ventral striatum and medial prefrontal cortex as a biomarker for stress-related psychopathology: Understanding interactive effects of early and more recent stress. *Psychological Medicine*, *23*, 1–9. https://doi.org/10.1017/S0033291717003348

Hanson, J. L., Williams, A. V., Bangasser, D. A., & Peña, C. J. (2021). Impact of Early Life Stress on Reward Circuit Function and Regulation. *Frontiers in Psychiatry*, *12*, 1799. https://doi.org/10.3389/fpsyt.2021.744690

Hodes, G. E., Pfau, M. L., Purushothaman, I., Ahn, H. F., Golden, S. A., Christoffel, D. J., Magida, J., Brancato, A., Takahashi, A., Flanigan, M. E., Menard, C., Aleyasin, H., Koo, J. W., Lorsch, Z. S., Feng, J., Heshmati, M., Wang, M., Turecki, G., Neve, R., … Russo, S. J. (2015). Sex Differences in Nucleus Accumbens Transcriptome Profiles Associated with Susceptibility versus Resilience to Subchronic Variable Stress. *Journal of Neuroscience*, *35*(50), 16362–16376. https://doi.org/10.1523/JNEUROSCI.1392-15.2015

Johnson, E. M., Kinoshita, Y., Weinreb, D. B., Wortman, M. J., Simon, R., Khalili, K., Winckler, B., & Gordon, J. (2006). Role of Purα in targeting mRNA to sites of translation in hippocampal neuronal dendrites. *Journal of Neuroscience Research*, *83*(6), 929–943. https://doi.org/10.1002/jnr.20806

Josselyn, S. A., Köhler, S., & Frankland, P. W. (2015). Finding the engram. *Nature Reviews Neuroscience*, *16*(9), 521–534. https://doi.org/10.1038/nrn4000

Kendler, K. S., Eaves, L. J., Loken, E. K., Pedersen, N. L., Middeldorp, C. M., Reynolds, C., Boomsma, D., Lichtenstein, P., Silberg, J., & Gardner, C. O. (2011). The impact of environmental experiences on symptoms of anxiety and depression across the life span. *Psychological Science*, *22*(10), 1343–1352. https://doi.org/10.1177/0956797611417255

Kessler, R. C., McLaughlin, K. A., Green, J. G., Gruber, M. J., Sampson, N. A., Zaslavsky, A. M., Aguilar-Gaxiola, S., Alhamzawi, A. O., Alonso, J., Angermeyer, M., Benjet, C., Bromet, E., Chatterji, S., de Girolamo, G., Demyttenaere, K., Fayyad, J., Florescu, S., Gal, G., Gureje, O., … Williams, D. R. (2010). Childhood adversities and adult psychopathology in the WHO World Mental Health Surveys. *The British Journal of Psychiatry : The Journal of Mental Science*, *197*(5), 378–385. https://doi.org/10.1192/bjp.bp.110.080499

Khalili, K., Del Valle, L., Muralidharan, V., Gault, W. J., Darbinian, N., Otte, J., Meier, E., Johnson, E. M., Daniel, D. C., Kinoshita, Y., Amini, S., & Gordon, J. (2003). Purα Is Essential for Postnatal Brain Development and Developmentally Coupled Cellular Proliferation As Revealed by Genetic Inactivation in the Mouse. *Molecular and Cellular Biology*, *23*(19), 6857–6875. https://doi.org/10.1128/MCB.23.19.6857-6875.2003

Kirshenbaum, J. S., Pagliaccio, D., Pizzagalli, D. A., & Auerbach, R. P. (2024). Neural sensitivity following stress predicts anhedonia symptoms: A 2-year multi-wave, longitudinal study. *Translational Psychiatry*, *14*(1), 1–9. https://doi.org/10.1038/s41398-024-02818-x

Kos, A., Lopez, J. P., Bordes, J., de Donno, C., Dine, J., Brivio, E., Karamihalev, S., Luecken, M. D., Almeida-Correa, S., Gasperoni, S., Dick, A., Miranda, L., Büttner, M., Stoffel, R., Flachskamm, C., Theis, F. J., Schmidt, M. V., & Chen, A. (2023). Early life adversity shapes social subordination and cell type–specific transcriptomic patterning in the ventral hippocampus. *Science Advances*, *9*(48), eadj3793. https://doi.org/10.1126/sciadv.adj3793

Kronman, H., Torres-Berrío, A., Sidoli, S., Issler, O., Godino, A., Ramakrishnan, A., Mews, P., Lardner, C. K., Parise, E. M., Walker, D. M., van der Zee, Y. Y., Browne, C. J., Boyce, B. F., Neve, R., Garcia, B. A., Shen, L., Peña, C. J., & Nestler, E. J. (2021). Long-term behavioral and cell-type-specific molecular effects of early life stress are mediated by H3K79me2 dynamics in medium spiny neurons. *Nature Neuroscience*, 1–10. https://doi.org/10.1038/s41593-021-00814-8

Kusiak, A., & Brady, G. (2022). Bifurcation of signalling in human innate immune pathways to NF-kB and IRF family activation. *Biochemical Pharmacology*, *205*, 115246. https://doi.org/10.1016/j.bcp.2022.115246

Lämke, J., & Bäurle, I. (2017). Epigenetic and chromatin-based mechanisms in environmental stress adaptation and stress memory in plants. *Genome Biology*, *18*(1), 124. https://doi.org/10.1186/s13059-017-1263-6

Lepack, A. E., Bagot, R. C., Peña, C. J., Loh, Y.-H. E., Farrelly, L. A., Lu, Y., Powell, S. K., Lorsch, Z. S., Issler, O., Cates, H. M., Tamminga, C. A., Molina, H., Shen, L., Nestler, E. J., Allis, C. D., & Maze, I. (2016). Aberrant H3.3 dynamics in NAc promote vulnerability to depressive-like behavior.

Proceedings of the National Academy of Sciences, *113*(44), 12562–12567. https://doi.org/10.1073/pnas.1608270113

Li, D., Hsu, S., Purushotham, D., Sears, R. L., & Wang, T. (2019). WashU Epigenome Browser update 2019. *Nucleic Acids Research*, *47*(W1), W158–W165. https://doi.org/10.1093/nar/gkz348

Marco, A., Meharena, H. S., Dileep, V., Raju, R. M., Davila-Velderrain, J., Zhang, A. L., Adaikkan, C., Young, J. Z., Gao, F., Kellis, M., & Tsai, L.-H. (2020). Mapping the epigenomic and transcriptomic interplay during memory formation and recall in the hippocampal engram ensemble. *Nature Neuroscience*, *23*(12), 1606–1617. https://doi.org/10.1038/s41593-020-00717-0

Martin, E. W., Krietsch, J., Reggiardo, R. E., Sousae, R., Kim, D. H., & Forsberg, E. C. (2021). Chromatin accessibility maps provide evidence of multilineage gene priming in hematopoietic stem cells. *Epigenetics & Chromatin*, *14*(1), 2. https://doi.org/10.1186/s13072-020-00377-1

McLaughlin, K. A., Conron, K. J., Koenen, K. C., & Gilman, S. E. (2010). Childhood adversity, adult stressful life events, and risk of past-year psychiatric disorder: A test of the stress sensitization hypothesis in a population-based sample of adults. *Psychological Medicine*, *40*(10), 1647–1658. https://doi.org/10.1017/S0033291709992121

Mo, A., Mukamel, E. A., Davis, F. P., Luo, C., Henry, G. L., Picard, S., Urich, M. A., Nery, J. R., Sejnowski, T. J., Lister, R., EDDY, S. R., Ecker, J. R., & Nathans, J. (2015). Epigenomic Signatures of Neuronal Diversity in the Mammalian Brain. *Neuron*, *86*(6), 1369–1384. https://doi.org/10.1016/j.neuron.2015.05.018

Moore, J. E., Purcaro, M. J., Pratt, H. E., Epstein, C. B., Shoresh, N., Adrian, J., Kawli, T., Davis, C. A., Dobin, A., Kaul, R., Halow, J., Van Nostrand, E. L., Freese, P., Gorkin, D. U., Shen, Y., He, Y., Mackiewicz, M., Pauli-Behn, F., Williams, B. A., … Weng, Z. (2020). Expanded encyclopaedias of DNA elements in the human and mouse genomes. *Nature*, *583*(7818), 699–710. https://doi.org/10.1038/s41586-020-2493-4

Moriceau, S., Roth, T. L., & Sullivan, R. M. (2010). Rodent model of infant attachment learning and stress. *Developmental Psychobiology*, *52*(7), 651–660. https://doi.org/10.1002/dev.20482

Muir, J., Tse, Y. C., Iyer, E. S., Biris, J., Cvetkovska, V., Lopez, J., & Bagot, R. C. (2020). Ventral Hippocampal Afferents to Nucleus Accumbens Encode Both Latent Vulnerability and Stress-Induced Susceptibility. *Biological Psychiatry*, *0*(0). https://doi.org/10.1016/j.biopsych.2020.05.021

Nord, A. S., & West, A. E. (2020). Neurobiological functions of transcriptional enhancers. *Nature Neuroscience*, *23*(1), 5–14. https://doi.org/10.1038/s41593-019-0538-5

O'Connor, T., Grant, C. E., Bodén, M., & Bailey, T. L. (2020). T-Gene: Improved target gene prediction. *Bioinformatics*, *36*(12), 3902–3904. https://doi.org/10.1093/bioinformatics/btaa227

Ong, C.-T., & Corces, V. G. (2014). CTCF: an architectural protein bridging genome topology and function. *Nature Reviews Genetics*, *15*(4), 234–246. https://doi.org/10.1038/nrg3663

Peña, C. J. (2017). D1 and D2 Type Medium Spiny Neuron Contributions to Depression. *Biological Psychiatry*, *81*(8), 636–638. https://doi.org/10.1016/j.biopsych.2017.02.010

Peña, C. J., Kronman, H. G., Walker, D. M., Cates, H. M., Bagot, R. C., Purushothaman, I., Issler, O., Loh, Y.-H. E., Leong, T., Kiraly, D. D., Goodman, E., Neve, R. L., Shen, L., & Nestler, E. J. (2017). Early life stress confers lifelong stress susceptibility in mice via ventral tegmental area OTX2. *Science*, *356*(6343), 1185–1188. https://doi.org/10.1126/science.aan4491

Peña, C. J., Nestler, E. J., & Bagot, R. C. (2019). Environmental Programming of Susceptibility and Resilience to Stress in Adulthood in Male Mice. *Frontiers in Behavioral Neuroscience*, *13*, 272. https://doi.org/10.3389/fnbeh.2019.00040

Peña, C. J., Smith, M., Ramakrishnan, A., Cates, H. M., Bagot, R. C., Kronman, H. G., Patel, B., Chang, A. B., Purushothaman, I., Dudley, J., Morishita, H., Shen, L., & Nestler, E. J. (2019). Early life stress alters transcriptomic patterning across reward circuitry in male and female mice. *Nature Communications*, *10*(1), Article 1. https://doi.org/10.1038/s41467-019-13085-6

Rakesh, D., Whittle, S., Sheridan, M. A., & McLaughlin, K. A. (2023). Childhood socioeconomic status and the pace of structural neurodevelopment: Accelerated, delayed, or simply different? *Trends in Cognitive Sciences*. https://doi.org/10.1016/j.tics.2023.03.011

Ramirez, M., Badayeva, Y., Yeung, J., Wu, J., Abdalla-Wyse, A., Yang, E., FANTOM 5 Consortium, Trost, B., Scherer, S. W., & Goldowitz, D. (2022). Temporal analysis of enhancers during mouse cerebellar development reveals dynamic and novel regulatory functions. *eLife*, *11*, e74207. https://doi.org/10.7554/eLife.74207

Reh, R. K., Dias, B. G., Nelson, C. A., Kaufer, D., Werker, J. F., Kolb, B., Levine, J. D., & Hensch, T. K. (2020). Critical period regulation across multiple timescales. *Proceedings of the National Academy of Sciences*, 201820836. https://doi.org/10.1073/pnas.1820836117

Reiff, S. B., Schroeder, A. J., Kırlı, K., Cosolo, A., Bakker, C., Mercado, L., Lee, S., Veit, A. D., Balashov, A. K., Vitzthum, C., Ronchetti, W., Pitman, K. M., Johnson, J., Ehmsen, S. R., Kerpedjiev, P., Abdennur, N., Imakaev, M., Öztürk, S. U., Çamoğlu, U., … Park, P. J. (2022). The 4D Nucleome Data Portal as a resource for searching and visualizing curated nucleomics data. *Nature Communications*, *13*(1), 2365. https://doi.org/10.1038/s41467-022-29697-4

Rincón-Cortés, M., & Sullivan, R. M. (2014). Early life trauma and attachment: Immediate and enduring effects on neurobehavioral and stress axis development. *Frontiers in Endocrinology*, *5*, 33. https://doi.org/10.3389/fendo.2014.00033

Russo, S. J., & Nestler, E. J. (2013). The brain reward circuitry in mood disorders. *Nature Reviews Neuroscience*, *14*(9), 609–625. https://doi.org/10.1038/nrn3381

Savell, K. E., Tuscher, J. J., Zipperly, M. E., Duke, C. G., Phillips, R. A., Bauman, A. J., Thukral, S., Sultan, F. A., Goska, N. A., Ianov, L., & Day, J. J. (2020). A dopamine-induced gene expression signature regulates neuronal function and cocaine

response. *Science Advances*, *6*(26), eaba4221. https://doi.org/10.1126/sciadv.aba4221

Saxton, K., & Chyu, L. (2019). Early life adversity increases the salience of later life stress: An investigation of interactive effects in the PSID. *Journal of Developmental Origins of Health and Disease*, *147*, 1–12. https://doi.org/10.1017/S2040174419000308

Schoenfelder, S., & Fraser, P. (2019). Long-range enhancer–promoter contacts in gene expression control. *Nature Reviews Genetics*, *20*(8), 437–455. https://doi.org/10.1038/s41576-019-0128-0

Schoenherr, C. J., & Anderson, D. J. (1995). The Neuron-Restrictive Silencer Factor (NRSF): A Coordinate Repressor of Multiple Neuron-Specific Genes. *Science*, *267*(5202), 1360–1363. https://doi.org/10.1126/science.7871435

Scott, K. M., McLaughlin, K. A., Smith, D. A. R., & Ellis, P. M. (2012). Childhood maltreatment and DSM-IV adult mental disorders: Comparison of prospective and retrospective findings. *The British Journal of Psychiatry*, *200*(6), 469–475. https://doi.org/10.1192/bjp.bp.111.103267

Sidamon-Eristoff, A. E., Cohodes, E. M., Gee, D. G., & Peña, C. J. (2022). Trauma exposure and mental health outcomes among Central American and Mexican children held in immigration detention at the United States–Mexico border. *Developmental Psychobiology*, *64*(1), e22227. https://doi.org/10.1002/dev.22227

Sisk, L. M., Keding, T. J., Cohodes, E. M., McCauley, S., Pierre, J. C., Odriozola, P., Kribakaran, S., Haberman, J. T., Zacharek, S. J., Hodges, H. R., Caballero, C., Gold, G., Huang, A. Y., Talton, A., & Gee, D. G. (2023). *Multivariate links between the developmental timing of adversity exposure and white matter tract integrity in adulthood* (p. 2023.11.12.566271). bioRxiv. https://doi.org/10.1101/2023.11.12.566271

Stroud, H., Yang, M. G., Tsitohay, Y. N., Davis, C. P., Sherman, M. A., Hrvatin, S., Ling, E., & Greenberg, M. E. (2020). An Activity-Mediated Transition in Transcription in Early Postnatal Neurons. *Neuron*. https://doi.org/10.1016/j.neuron.2020.06.008

Sun, W., Liu, Z., Jiang, X., Chen, M. B., Dong, H., Liu, J., Südhof, T. C., & Quake, S. R. (2024). Spatial transcriptomics reveal neuron–astrocyte synergy in long-term memory. *Nature*, 1–8. https://doi.org/10.1038/s41586-023-07011-6

Taniguchi, T., Ogasawara, K., Takaoka, A., & Tanaka, N. (2001). IRF Family of Transcription Factors as Regulators of Host Defense. *Annual Review of Immunology*, *19*(Volume 19, 2001), 623–655. https://doi.org/10.1146/annurev.immunol.19.1.623

Torres-Berrío, A., Estill, M., Ramakrishnan, A., Kronman, H., Patel, V., Minier-Toribio, A., Issler, O., Browne, C. J., Parise, E. M., Van Der Zee, Y., Walker, D., Martínez-Rivera, F. J., Lardner, C. K., Cuttoli, R. D., Russo, S. J., Shen, L., Sidoli, S., & Nestler, E. J. (2023). Monomethylation of Lysine 27 at Histone 3 Confers Lifelong Susceptibility to Stress. *bioRxiv*. https://doi.org/10.1101/2023.05.08.539829

UNICEF. (2018). Child Displacement. *UNICEF*. https://data.unicef.org/topic/child-migration-and-displacement/displacement/

Vicente-Dueñas, C., Hauer, J., Cobaleda, C., Borkhardt, A., & Sánchez-García, I. (2018). Epigenetic Priming in Cancer Initiation. *Trends in Cancer*, *4*(6), 408–417. https://doi.org/10.1016/j.trecan.2018.04.007

Wang, H., Xiao, Z., Zheng, J., Wu, J., Hu, X.-L., Yang, X., & Shen, Q. (2019). ZEB1 Represses Neural Differentiation and Cooperates with CTBP2 to Dynamically Regulate Cell Migration during Neocortex Development. *Cell Reports*, *27*(8), 2335-2353.e6. https://doi.org/10.1016/j.celrep.2019.04.081

Webb, E. K., Carter, S. E., Ressler, K. J., Fani, N., & Harnett, N. G. (2024). The neurophysiological consequences of racism-related stressors in Black Americans. *Neuroscience & Biobehavioral Reviews*, *161*, 105638. https://doi.org/10.1016/j.neubiorev.2024.105638

Wu, W.-S., You, R.-I., Cheng, C.-C., Lee, M.-C., Lin, T.-Y., & Hu, C.-T. (2017). Snail collaborates with EGR-1 and SP-1 to directly activate transcription of MMP 9 and ZEB1. *Scientific Reports*, *7*(1), 17753. https://doi.org/10.1038/s41598-017-18101-7

Wurst, W., & Prakash, N. (2014). Wnt1-regulated genetic networks in midbrain dopaminergic neuron development. *Journal of Molecular Cell Biology*, *6*(1), 34–41. https://doi.org/10.1093/jmcb/mjt046

Yohn, C., Dieterich, A., Bazer, A., Maita, I., Giedraitis, M., & Samuels, B. (2019). Chronic Non-Discriminatory Social Defeat Is an Effective Chronic Stress Paradigm for Both Male and Female Mice. *Neuropsychopharmacology*, *44*(13), 2220–2229. https://doi.org/10.1038/s41386-019-0520-7

Zachry, J. E., Kutlu, M. G., Yoon, H. J., Leonard, M. Z., Chevée, M., Patel, D. D., Gaidici, A., Kondev, V., Thibeault, K. C., Bethi, R., Tat, J., Melugin, P. R., Isiktas, A. U., Joffe, M. E., Cai, D. J., Conn, P. J., Grueter, B. A., & Calipari, E. S. (2024). D1 and D2 medium spiny neurons in the nucleus accumbens core have distinct and valence-independent roles in learning. *Neuron*, *112*(5), 835-849.e7. https://doi.org/10.1016/j.neuron.2023.11.023

Zhang, Z.-Y., Mao, Y., Feng, X.-L., Zheng, N., Lü, L.-B., Ma, Y.-Y., Qin, D.-D., & Hu, X.-T. (2016). Early adversity contributes to chronic stress induced depression-like behavior in adolescent male rhesus monkeys. *Behavioural Brain Research*, *306*, 154–159. https://doi.org/10.1016/j.bbr.2016.03.040